SosA inhibits cell division in *Staphylococcus aureus* in response to DNA damage

Martin S. Bojer[a,b], Katarzyna Wacnik[c], Peter Kjelgaard[a], Clement Gallay[d], Amy L. Bottomley[c,*], Marianne T. Cohn[a], Gunnar Lindahl[a], Dorte Frees[a], Jan-Willem Veening[d], Simon J. Foster[c] & Hanne Ingmer[a,b,#]

[a]Department of Veterinary and Animal Sciences, Faculty of Health and Medical Sciences, University of Copenhagen, Copenhagen, Denmark.

[b]Centre for Bacterial Stress Response and Persistence, University of Copenhagen, Copenhagen, Denmark.

[c]The Krebs Institute, Department of Molecular Biology and Biotechnology, University of Sheffield, Sheffield, United Kingdom.

[d]Department of Fundamental Microbiology, University of Lausanne, Lausanne, Switzerland.

[*]Present address: The ithree Institute, University of Technology Sydney, Sydney, NSW, Australia.

Short title: SosA inhibits *S. aureus* cell division

Key words: *Staphylococcus aureus*, cell division, SOS response, cell-division inhibition, SosA, DivIC, PBP1, CtpA.

[#]Corresponding author: Hanne Ingmer; Stigbøjlen 4, 1870 Frederiksberg, Denmark; Telephone: +45 2215 9518; email: hi@sund.ku.dk

Abstract

Inhibition of cell division is critical for cell viability under DNA damaging conditions. In bacterial cells, DNA damage induces the SOS response, a process that inhibits cell division while repairs are being made. In coccoid bacteria, such as the human pathogen *Staphylococcus aureus*, the process remains poorly understood. Here we have characterized an SOS-induced cell-division inhibitor, SosA, in *S. aureus*. We find that in contrast to the wildtype, *sosA* mutant cells continue division under DNA damaging conditions with decreased viability as a consequence. Conversely, overproduction of SosA leads to cell division inhibition and reduced growth. The SosA protein is localized in the bacterial membrane and mutation of an extracellular amino acid, conserved between homologs of other staphylococcal species, abolished the inhibitory activity as did truncation of the C-terminal 30 amino acids. In contrast, C-terminal truncation of 10 amino acids lead to SosA accumulation and a strong cell division inhibitory activity. A similar phenotype was observed upon expression of wildtype SosA in a mutant lacking the membrane protease, CtpA. Thus, the extracellular C-terminus of SosA is required both for cell-division inhibition and for turnover of the protein. Functional studies showed that SosA is likely to interact with one or more divisome components and, without interfering with early cell-division events, halts cell division at a point where septum formation is initiated yet being unable to progress to septum closure. Our findings provide important insights into cell-division regulation in staphylococci that may foster development of new classes of antibiotics targeting this essential process.

39 **Importance**

40 *Staphylococcus aureus* is a serious human pathogen and a model organism for cell-division studies
41 in spherical bacteria. We show that SosA is the DNA-damage-inducible cell-division inhibitor in *S.*
42 *aureus* that upon expression causes cell swelling and cessation of the cell cycle at a characteristic
43 stage post septum initiation but prior to division plate completion. SosA appears to function via an
44 extracellular activity and is likely to do so by interfering with the essential membrane-associated
45 division proteins, while at the same time being negatively regulated by the membrane protease
46 CtpA. This report represents the first description of the process behind cell-division inhibition in
47 coccoid bacteria. As several pathogens are included in this category, uncovering the molecular
48 details of SosA activity and control can lead to identification of new targets for development of
49 valuable anti-bacterial drugs.

50

51 **Introduction**

52 Bacteria multiply by coordinated and essential DNA replication and cell-division events, two
53 important biological processes that are valuable targets for antimicrobial therapy (1-4). In the
54 event of DNA damage, the SOS response is activated and ensures that cell division is delayed until
55 the DNA is repaired. The SOS regulon is controlled by the conserved LexA repressor, which is
56 inactivated in response to RecA, a sensor of DNA damage at stalled replication forks, binding to
57 single-stranded DNA (5-7). The SOS response has mostly been studied in *Escherichia coli*, a gram-
58 negative rod-shaped bacterium where the LexA-regulated gene, *sulA*, encodes a cell-division
59 inhibitor. This inhibitor suppresses division by binding to FtsZ, which acts as a scaffold for the

60 assembly of cell-division components at the division site (4, 8-13). In rod-shaped bacteria,
61 inhibition of cell division leads to filamentation as a consequence of lateral peptidoglycan
62 synthesis. This phenotype is also observed in *E. coli* mutants lacking the Lon protease of which
63 SulA is a substrate, further substantiating the role of SulA in cell-division inhibition and
64 filamentation (14, 15).

65 SulA is poorly conserved in species outside Enterobacteriaceae. The α-proteobacterium
66 *Caulobacter crescentus* encodes an SOS-induced cell-division inhibitor SidA that does not show
67 homology to SulA. In contrast to cytosolic SulA, SidA is a membrane-anchored, small protein that
68 does not interact with FtsZ but rather with later cell-division proteins (16). In this species, yet
69 another, possibly redundant, cell-division inhibitor DidA is implicated in survival during DNA
70 damage, while being independent on the SOS response (17). Hence, it appears that bacteria
71 choose fundamentally different ways to orchestrate regulated cell-division inhibition in response
72 to DNA damage. For gram-positive, spherical cells such as *Staphylococcus aureus*, however, little is
73 known of how SOS induction is coupled to cell division nor have specific posttranslational
74 mechanisms for the negative regulation of cell-division inhibition been identified.

75 *S. aureus* is a serious gram-positive human pathogen, notorious for being implicated in a wide
76 range of infections and for being able to acquire resistance towards important antibiotic classes. It
77 originally received its name from the grape-like clusters of coccoid cells that result from the
78 unique cell-division process that occurs in three consecutive orthogonal planes (18-20). In this
79 organism, we and others have previously identified *lexA* and noted an open reading frame
80 (designated *sosA*) that is divergently transcribed from *lexA* and controlled by the LexA repressor
81 and the SOS response (21-24). The location of *sosA* adjacent to *lexA* indicated that it might encode

82 a cell-division inhibitor, as similar gene synteny has been observed for SOS-induced, cell-division
83 inhibitors encoded by gram-positive, rod-shaped bacteria, namely *Bacillus subtilis* (25), *Bacillus*
84 *megaterium* (26), *Listeria monocytogenes* (27, 28), *Mycobacterium tuberculosis* (29), and
85 *Corynebacterium glutamicum* (30) (Fig. 1A). The cell-division inhibitors of these organisms display
86 no similarity to SulA, and within the group they generally show little homology with the exceptions
87 of YneA from *L. monocytogenes* and ChiZ from *M. tuberculosis* (29) that resemble *B. subtilis* YneA.
88 Commonly, however, they have a single membrane spanning segment, a predicted extracellular C-
89 terminus and, except for DivS from *C. glutamicum*, a LysM domain, which is a ubiquitous
90 peptidoglycan binding motif (31, 32), suggesting that membrane and/or cell-wall localization is a
91 common feature characterizing gram-positive cell-division inhibitors.

92 The fundamental processes of staphylococcal cell division have been studied spatiotemporally
93 using super-resolution microscopy techniques (19, 33), and recent efforts combining genetic
94 approaches have unveiled the molecular mechanism in unprecedented detail (34, 35). Here, we
95 demonstrate that *sosA* encodes the SOS-inducible cell-division inhibitor in *S. aureus* and document
96 its impact on cell division following treatment with DNA damaging agents. Moreover, we identify a
97 possible mechanism for the proteolytic control of endogenous cell-division inhibition. Thus, we
98 further our insight into these basic biological phenomena, which could lead to the development of
99 new antimicrobials targeting the cell-division machinery in *S. aureus*.

100

101

102

103 ## Results

104 **Conservation of *sosA* in staphylococci.** In *S. aureus*, the open reading frame located adjacent to
105 *lexA* (divergently transcribed) was named *sosA* and hypothesized to encode an inhibitor of cell
106 division (Fig. 1A) (23). The 77-amino-acid-long product has homology and 25-60% amino-acid
107 identity to proteins encoded by genes occupying the same chromosomal location in a range of
108 staphylococci (Fig. 1B and Fig. S1), while showing no clear homology to the known gram-positive
109 cell-division inhibitors. Of note, the C-terminal part of SosA lacks a LysM domain, which is present
110 in the cell-division inhibitors YneA and ChiZ (36, 37). The N-terminal half of SosA includes a
111 putative transmembrane (TM) domain, and the C-terminal part is predicted to be located
112 extracellularly (TOPCONS server [38]). Among the different staphylococcal species, a highly
113 conserved sequence is located just C-terminally of the predicted TM domain and, although less
114 striking, some conservation also seems to exist in the extreme C-terminus (Fig. 1B).

115 **Genotoxic stress inhibits cell division in an SosA-dependent manner.** To analyze whether SosA
116 serves as an SOS-induced cell-division inhibitor, we exposed 8325-4, the common laboratory *S.*
117 *aureus* strain, and JE2, a derivative of the clinically relevant USA300 lineage, to a lethal
118 concentration of the DNA damaging agent Mitomycin C (MMC) and observed induction of SosA
119 expression in both strains by western blot analysis (Fig. S2A). In contrast, no SosA was observed in
120 deletion mutant derivatives but was expressed in a complemented strain. (Fig. S2A). Upon
121 exposure to the same lethal dose of MMC for a 2 hour period, wildtype cells showed 10-100-fold
122 greater survival than the mutant cells lacking SosA, whereas the optical densities of both cell type
123 cultures were comparable (Fig. 2A). Flow cytometry measurements of cell size distributions
124 revealed that treatment with MMC led to a three- and six-fold increase in forward light scatter

125 (FSC-A) values in 8325-4 and JE2, respectively, while the cell size distribution of the mutants
126 lacking *sosA* remained essentially constant (Fig. 2B). The constant cell size but increasing optical
127 densities of the *sosA* mutant populations implies that during DNA damage these cells, in contrast
128 to wildtype cells, continue to divide. Indeed, this striking phenotype was confirmed by time-lapse
129 microscopy, where wildtype cells increased in size over time, occasionally growing so large that
130 lysis occurred, while the size of the mutant cells lacking *sosA* stayed the same and cell division
131 continued (Fig. 2C and Movie S1). The phenotypes of the 8325-4 *sosA* mutant were abrogated in a
132 strain complemented with a chromosomal copy of *sosA* expressed from its native promoter (Fig.
133 S2B and C). Thus, SosA seems to prevent or delay cell division; maintain viability of *S. aureus* under
134 DNA damaging conditions, and as a consequence of continued peptidoglycan synthesis cause cell
135 size to increase.

136 **SosA overexpression inhibits cell division.** If SosA is indeed a cell-division inhibitor in *S. aureus*, it
137 can be predicted that overexpression of the protein should be sufficient to inhibit growth even
138 under conditions with no DNA damage. Hence, we expressed *sosA* episomally from an
139 anhydrotetracycline (AHT)-inducible promoter and found that while the control vector did not
140 affect cell viability, the plating efficiency of cells carrying the *sosA* overexpression plasmid was
141 markedly compromised under inducing conditions (Fig. 3A). When grown in liquid culture and
142 compared to the control, the SosA overexpressing cells showed a 2-3-fold increase in forward light
143 scatter values, reflecting that the size of the *sosA*-expressing cells increased (Fig. 3B). Microscopy
144 observations over time confirmed the slight increase in cell size and the reduction in the overall
145 number of cells upon SosA overproduction (Fig. 3C and Movie S2). Interestingly, contrary to what
146 was observed under DNA-damaging conditions (Fig. 2B), we found that ectopic induction of SosA

147 caused only a transient increase in cell size (compare time points 45 and 90 min to 135 min in Fig.
148 3B), indicating the existence of a negative regulatory mechanism.

149 **The C-terminal part of SosA is functionally essential and possibly required for autoregulation.**
150 The C-terminal part of SosA contains segments that appear somewhat conserved in staphylococci
151 (Fig. 1B), and *in silico* it is predicted to be extracellular. First, we confirmed its extracellular
152 location by constructing PhoA-LacZ reporter fusions (39), whereby a fusion of the reporter
153 chimera to the C-terminus of SosA conferred a phosphatase-positive, β-galatosidase-negative
154 phenotype in *E. coli*, indicative of translocation across the membrane (Fig. 4). Next, aiming at a
155 functional characterization of its role in SosA activity, we constructed a series of C-terminally
156 truncated variants by the successive elimination of ten amino acids (AAs), resulting in four variants
157 of SosA lacking between 10 and 40 of the C-terminal AAs (Fig. 5A). Strikingly, we observed that
158 truncation of the 10 C-terminal AAs (and to some extent also removal of 20 C-terminal AAs)
159 strongly compromised plating efficiency even at low inducer concentrations (Fig. 5B). Time-lapse
160 microscopy revealed that cells producing SosAd10 (SosA missing the last 10 AAs) had a dramatic
161 phenotype, with prominent cell swelling and a reduction of the cell-cycle rate (Fig. 5C and Movie
162 S3). The phenotypes from the plating assay correlated with the cell size measurements by flow
163 cytometry (Fig. S2D). These results indicate that cells expressing the 10 AA truncated protein are
164 stalled in a non-dividing state leading to abnormal cell size, whereas those expressing full-length
165 SosA are only transiently halted or delayed in cell division (Fig. S2D and Movie S3). In contrast,
166 deletion of 30 or 40 AAs from the C-terminal part eliminated the ability of SosA to inhibit cell
167 division, as cells expressing SosAd30 or SosAd40 gave comparable plating efficiency as those
168 carrying the vector (Fig. 5B) and caused no effect on cell size upon induction (Fig. S2D). This
169 prompted us to investigate the relevance of the highly conserved residues located in the

170 membrane-proximal part of the SosA C-terminal part by performing alanine substitutions within
171 the protein. To this end, we used the highly inhibitory SosAd10 variant as a scaffold and found that
172 while point mutations at AA positions 37 or 38 (E and Q) had no effect, point mutations at
173 positions 40 or 41 (Y and E) partially inactivated and the mutations at positions 44 and 45 (D and
174 H) completely abolished the cell-division inhibitory activity of the protein (Fig. 6A). The mutation
175 at AA position 44 (D to A) was subsequently shown also inactivate the inhibitory activity of the full-
176 length protein (Fig. 6B). Importantly, the inactive variants SosAd40 and SosAd10(44A) are still
177 likely to be localized in the membrane, as are SosA and SosAd10, when evaluated by the PhoA-
178 LacZ translocation assay (Fig. 4). We conclude that conserved residues in the membrane-proximal
179 segment of the extracellular C-terminal part of SosA are essential for inhibiting cell division, while
180 truncation at the extreme C-terminus of the protein augments activity.

181 **A CtpA protease mutant is hypersusceptible to SosA expression.** We reasoned that one
182 explanation for the severe impact of the 10-AA-truncated SosA on cell division could be that the
183 extreme C-terminus of SosA serves as an endogenous signal for proteolytic degradation, and its
184 removal allows the mutant protein to escape degradation and accumulate. Indeed, we observed
185 that the cellular accumulation of the truncated protein was higher than for the wildtype protein
186 following one hour of ectopic expression (Fig. S2E). In parallel, we observed the same pattern for
187 cells expressing the 10-AA-truncated SosA variant with the 44A mutation that abolishes the cell
188 division inhibitory activity suggesting that the phenotype of the mutation is not related to
189 instability of the SosA variant (Fig. S2E). To identify a membrane localized protease that may be
190 responsible for SosA turn-over we searched the Nebraska Transposon Mutant Library (40) for *S.*
191 *aureus* protease mutant strains, and as a potential candidate, we identified the carboxyl-terminal
192 protease A, CtpA. The *S. aureus* CtpA protein is located at the cell-membrane/cell-wall fraction

193 and is involved in stress tolerance and virulence in a mouse model of infection (41). Importantly,
194 overproduction of the wildtype SosA protein in cells lacking *ctpA* completely abolished cell
195 viability, similarly to what was observed when the 10-AA-truncated SosA protein was expressed in
196 wildtype *S. aureus* cells (Fig. 7A). In agreement with this result, we found that overproduction of
197 SosA and CtpA in the *ctpA* mutant background alleviated the detrimental effect of SosA and that
198 the degree of complementation depended on the relative expressional levels of the two proteins,
199 where higher expression level of SosA was only partially complemented by CtpA expression (Fig.
200 S3). Further substantiating the negative regulatory role played by CtpA with respect to SosA, we
201 noted that the *ctpA* mutant was substantially more sensitive to MMC (measured by plating
202 efficiency) than wildtype *S. aureus*, but only when encoding a functional *sosA* gene (Fig. 7B).
203 Additionally, upon MMC-induced DNA damage, higher levels of the SosA protein accumulated in
204 the *ctpA* mutant when compared to the wildtype (Fig. 7C). Importantly, parallel experiments were
205 recently reported showing that CtpA in *B. subtilis* is one of two proteolytic regulators of the cell-
206 division inhibitor YneA, with CtpA displaying direct proteolytic activity against the target in vitro.
207 (42) Altogether, based on these results, we propose that the extracellular C-terminus of SosA is a
208 substrate for CtpA proteolytic activity and that proteolysis relieves SosA-mediated cell-division
209 inhibition allowing growth to resume once DNA stress has ceased.

210 **SosA is a late-stage cell-division inhibitor.** To pinpoint at which step of the cell-division process
211 the SosA-mediated inhibition is taking place, we employed fluorescence microscopy to monitor
212 the cellular localization of FtsZ and EzrA, crucial early-stage cell-division proteins in *S. aureus*, upon
213 induction of SosA overproduction. Neither the *sosA* overexpression plasmid in non-inducing
214 conditions (Fig. 8A and B) nor the control vector in non-inducing or inducing conditions (Fig. S4A
215 and B) changed the cell morphology or protein localization. As expected, SosA overexpression

216 caused cell swelling but also it did not cause de-localization of the cell-division initiator FtsZ (Fig.
217 8A) or affected the placement of the membrane-bound division protein EzrA (Fig. 8B), which is an
218 early recruited protein connecting the cytoplasmic division components with the peptidoglycan-
219 synthesizing membrane-bound complex (43). What was evident, however, was that whereas
220 wildtype cells are heterogeneous with respect to FtsZ localization due to their presence in
221 different phases of cell division, *sosA*-expressing cells appear highly synchronized with FtsZ
222 preferentially showing septal localization (compare uninduced and induced cells in Fig. 8A)

223 To further explore the cellular consequences of SosA-mediated cell-division inhibition, we
224 examined the phenotypes of JE2/pSosA cells that were labeled for five minutes with HADA,
225 marking regions of nascent peptidoglycan synthesis, and grown in the absence or presence of
226 SosA induction (Fig. S4C). While in the absence of AHT, 47% and 23% of cells, respectively, showed
227 a ring (incomplete septum) or line (complete septum) of nascent peptidoglycan synthesis, there
228 was accumulation (89%) of cells with incomplete septa and a severe drop in cells with complete
229 septa (1%) when SosA was overexpressed (Fig. 8C). Additionally, 1% of cells had an 'hourglass'
230 shape after incubation with AHT, indicative of non-productive, premature splitting taking place
231 prior to septum completion. Next, whole cell walls of cells overproducing SosA were labeled with a
232 fluorescent NHS ester and examined by 3D-structured illumination microscopy (3D-SIM).
233 Microscopy visualization revealed that most cells had only signs of septation — a so-called
234 'piecrust' (19) (Fig. S4Ei) — and showed that in an hourglass-like cell, there was a gap in the septal
235 peptidoglycan (Fig. S4Eii). The fact that SosA does not affect localization of early cell-division
236 proteins, FtsZ and EzrA, and the cell population becomes synchronized to a particular stage of the
237 cell cycle (phase P2 [33]) shows that SosA does not hinder the initiation of septum formation but
238 blocks the progression of septum completion — a phenotype similar to *S. aureus* DivIB-depleted

239 cells (44). Although DivIB has been shown to be dispensable for FtsZ and EzrA localization to the
240 septum and piecrust formation, its absence results in inhibition of septum progression and
241 completion and in the mislocalization of GpsB (44), a late cell-division protein (44, 45). However,
242 SosA overproduction did not impair the recruitment of GpsB to the mid-cell (Fig. 8D) even though
243 visible cell enlargement occurred in this reporter strain (Fig. 8D) and not in the vector control (Fig.
244 S4D). Altogether, these results indicate that SosA acts on (a) later cell-division component(s) than
245 FtsZ, EzrA, and GpsB, and we conclude that SosA causes a characteristic halt in cell division by
246 preventing progression through the morphological division stage P2, i.e. septum plate completion.

247 **Possible divisome interaction partners for SosA.** No direct interaction has been observed
248 between the gram-positive cell-division inhibitors and FtsZ, the scaffold for cell-division
249 components assembly at the division site. Though poorly characterized mechanistically, the gram-
250 positive inhibitors may suppress cell division at later stages, potentially by interacting with
251 FtsI/FtsQ (for *M. tuberculosis* ChiZ) as suggested by bacterial two-hybrid analysis (36) or via
252 delocalization of FtsL and/or DivIC (for *B. subtilis* YneA) which was only supported by indirect
253 experimental data (46). By employing a bacterial two-hybrid system approach that reports
254 protein-protein interactions, we sought to identify potential *in vivo* interaction candidates for SosA
255 based on cell-division proteins from *S. aureus* (43). This analysis indicated that PBP1 (penicillin-
256 binding protein 1), DivIC, and PBP3 are possible targets for the activity of SosA (Fig. 9A). PBP1 is a
257 homolog of *E. coli* FtsI (47) and an essential component of the divisome that, in *S. aureus*, is
258 considered to play a role in septum formation and cell separation, with only the latter activity
259 relying on transpeptidase (TP) activity of the enzyme (48). DivIC is part of an essential tripartite
260 complex, DivIB-FtsL-DivIC (FtsQLB in *E. coli*), considered part of the second recruitment to the
261 divisome (45, 49). Although displaying no enzymatic activity these proteins are mutually

262 dependent on each other for stability as well being required for assembly of the final synthetic
263 division machinery (49, 50). PBP3 is non-essential in *S. aureus* (51), but otherwise its localization
264 and function is unknown (20). If either of these proteins are indeed targets for SosA, we predicted
265 that ectopic expression of *pbpA* (encoding PBP1), *divIC*, or *pbpC* (encoding PBP3) would mitigate
266 the effect of concomitant SosA overexpression by increasing the level of target protein. While no
267 effect was observed upon DivIC and PBP3 co-overexpression, overproduction of PBP1 along with
268 SosA was manifested as a synergistically lethal phenotype with to considerable growth
269 impairment (Fig. 9B). Further, we found that this phenotype was apparent even at low inducer
270 concentrations, where the effect of SosA overproduction alone is negligible, and that it was
271 independent on the transpeptidase activity of PBP1 as overexpression of a mutant variant of PBP1
272 lacking this activity together with SosA still eliminated growth (Fig. S5A). The phenotype is,
273 however, dependent on the cell-division inhibitory activity of SosA as concomitant overproduction
274 of the SosA(44A) mutant protein abolished the phenotype (Fig. S5B), suggesting that the lethal
275 phenotype is not a simple artifact of ectopic overexpression of a membrane protein along with
276 PBP1. While these data do not support a simple titration of SosA by PBP1, it does support that
277 SosA is mechanistically linked to, or intercepts with the activity of PBP1. It is also conceivable that
278 SosA and PBP1 act synergistically on the same target protein, the former by inhibiting its activity
279 and the latter via disrupting the stoichiometry of the division components. Lastly, we examined
280 the importance of the inactivating mutation (44A) of SosA as well as the stabilizing (SosAd10) and
281 inactivating (SosAd40) truncations to the protein for interaction with PBP1 and DivIC, respectively.
282 Interestingly, we find that the inactivating mutation compromises interaction with DivIC only,
283 whereas both interactions are dependent on the C-terminus of SosA (Fig. 9C). This indicates that
284 the inhibitory activity of SosA is functionally related to its interaction with DivIC.

285 **Discussion**

286 Based on the results reported here, we propose the following model for regulation of cell division
287 in the prolate spheroid bacterium *S. aureus* under DNA-damaging conditions (Fig. 10). During
288 normal growth, the expression of *sosA* and the entire SOS regulon is repressed by the LexA
289 repressor. Under DNA damaging and SOS inducing conditions, LexA is inactivated through
290 autocleavage, which results in the expression of *sosA*. In this process, the N-terminal autocleavage
291 product of LexA needs to be further proteolytically processed for *sosA* expression to be fully
292 induced (23), thus adding another layer of expressional control, suggesting tight regulation of the
293 inhibitory protein. Upon derepression of LexA-regulated genes, SosA accumulates to levels that
294 inhibit cell division without causing FtsZ delocalization nor preventing the assembly of
295 downstream components, EzrA and GpsB, which are representatives of early and later cell division
296 components. The inhibitor appears to affect the progression and completion of septum formation
297 via interaction with essential divisome components with DivIC being one such possible target
298 candidate. As a consequence of SosA activity, the cells appear synchronized at the stage of septum
299 formation initiation, while an ongoing off-septal peptidoglycan synthesis leads to cell enlargement
300 (Fig. S4C). Once conditions are favorable for continued division, *sosA* expression is repressed, the
301 membrane protease CtpA degrades SosA, and cell division resumes (Fig. 10).

302 The model illuminates several remaining unanswered questions. It will be particularly important to
303 determine if and how SosA affects the function of DivIC and by which means SosA intercepts the
304 activity of PBP1. In this context, it should be noted that our data fit well with the finding that the
305 genetic depletion of PBP1 causes cell enlargement and incomplete septum formation (47). At
306 present we cannot readily explain the peculiar finding that SosA and PBP1 seem to act in a

307 synergistically lethal manner (Fig. 9, and Fig. S5). Though it is formally possible that the two
308 proteins together constitute a signal to halt septum formation beyond a certain point, it is
309 plausible that our observations are due to severe changes in stoichiometry within the divisome. It
310 is also conceivable that overexpression of PBP1 is prematurely forcing septum completion which
311 could be counterproductive under the inhibitory activity of SosA. In fact, we find that
312 overexpression of another essential component of the peptidoglycan synthesis machinery, the
313 lipid II flippase MurJ, is also synthetically lethal when SosA is expressed (Fig S5C), showing that the
314 phenotype is not exclusively related to PBP1. Our microscopy and localization data suggest that
315 SosA acts quite specifically at a decision point between septum initiation and septum completion.
316 In this regard, it is interesting that cell division in *S. aureus* was recently reported to be a two-step
317 process characterized by an initial, slow FtsZ-dependent activity followed by a faster process when
318 MurJ arrives and directs peptidoglycan synthesis to the septum (in division stage P2 where SosA
319 expressing cells are stalled) (35). More intriguingly, MurJ recruitment was reported to be mediated
320 by the DivIB-FtsL-DivIC complex (35), which could constitute an important molecular cue for the
321 inhibitory activity of SosA. Along this line, FtsL and DivIC are considered unstable proteins, and in
322 *B. subtilis* stability of DivIC is dependent on FtsL (52). Hence, we tried to co-express FtsL along with
323 SosA and did note a partial alleviation of the inhibitory activity (Fig. S5D). We take this observation
324 as another indication that DivIC could be a direct target of SosA, although at present we cannot
325 exclude indirect effects. Interactions between the *S. aureus* divisome components constitute a
326 complex web, and in a previous bacterial two-hybrid study it has been shown that PBP1 interacts
327 with DivIC, which in turn interacts with PBP3 (43). Thus, the inhibitory activity of SosA could be
328 multifactorial and further studies are required to delineate the exact function of the protein. Such
329 studies should include localization studies of e.g., DivIC and MurJ as recently employed (35) but

330 could also include mutational and suppressor studies as elegantly used to map the cell-division
331 inhibition process in *C. crescentus* (16, 17).

332 Analysis of the AA sequence of SosA indicated that the N-terminal part contains a TM domain
333 while the C-terminal is located extracellularly. The hypothesis that the TM domain promotes
334 localization to the cellular membrane was supported by PhoA-LacZ fusion to SosA and by various
335 point and deletion mutants of the fusion protein (Fig. 4). The abrogation of activity by the 40-AA-
336 truncation as well as by a single alanine substitution (D44A) suggests that this segment is essential
337 for correct localization to the septum or, perhaps more interestingly, that the actual motif for cell-
338 division inhibition is localized at the exterior of the membrane. In this respect, it is interesting that
339 the single amino acid substitution affects the interaction with DivIC in the two-hybrid system (Fig.
340 9C). If divisome interference indeed lies within this extracellular segment of SosA, it could provide
341 a novel paradigm for interference with cell-division beyond the transpeptidase-inhibitory activity
342 exerted by β-lactam antibiotics.

343 Endogenously triggered cell-division inhibition must be strictly regulated, as demonstrated by
344 pioneering work showing that SulA of *E. coli* is degraded by the Lon protease (15). Similarly, YneA
345 from *B. subtilis* was reported to be regulated by proteolysis, by an undefined mechanism, and a
346 point mutation at its extreme C-terminus generated a stabilized yet functional variant of the cell-
347 division inhibitor (37). In *B. megaterium*, the temporal expression of a YneA homologue has been
348 suggested to be due to mRNA instability (26). We demonstrate that a minor truncation of the C-
349 terminus of SosA increases cell division inhibitory activity (Fig. 5), possibly as a consequence of
350 accumulation of the protein (Fig. S2E). This led us to speculate that the extreme C-terminus serves
351 as a signal for proteolysis and we identified the CtpA protease-deficient strain in which SosA

352 appeared to accumulate and had an increased detrimental effect compared to the wildtype
353 background. Bacterial carboxy-terminal proteases are poorly characterized, particularly with
354 respect to their substrate preferences; however, we propose that CtpA specifically regulates SOS-
355 induced cell-division inhibition in staphylococci, likely via recognition of the C-terminus of SosA. In
356 support of this, Burby et al. (42) recently disclosed that CtpA is involved in turn-over of YneA in *B.*
357 *subtilis*. Direct biochemical evidence for such a direct activity of CtpA on SosA in *S. aureus* is
358 needed, but a shared mechanism is highly conceivable. Of note, carboxy-terminal proteases are
359 ubiquitous in bacterial genera, and homologs of CtpA are found in other gram-positive species,
360 including also *L. monocytogenes* which share a homolog of YneA. Hence, the CtpA-like proteases
361 could represent functional homologs of the *E. coli* Lon protease, allowing negative regulation of
362 membrane-localized endogenous cell-division inhibition more broadly amongst Firmicutes and
363 beyond.

364 SosA may also prove to be a useful tool for scientists conducting studies of bacterial cell division,
365 which have recently benefitted from the development of genetic tools and highly sophisticated
366 microscopic imaging technologies. However, most often bacteria grow as an unsynchronized
367 population with individual cells in different phases of cell division, making it challenging to order
368 the temporal events that occur during cell-cycle progression, DNA replication, and division.
369 Essentially, SosA is involved in halting the *S. aureus* cell cycle at a specific morphological stage, e.g.
370 following the piecrust formation, and we anticipate that the exploitation of this function may
371 constitute a useful tool for the generation of synchronized staphylococcal cells for experimental
372 purposes.

373 Apart from its basic biological interest, the bacterial cell-division process may constitute an
374 unexhausted source of novel therapeutic targets (1,2). We believe that SosA could be a natural
375 scaffold, and that further studies on this protein can provide new therapeutically accessible
376 targets that would interfere with an essential process in *S. aureus* and other staphylococci.

377

378 Materials and Methods

379 **Bacterial strains and plasmids used in this work.** The bacterial strains and plasmids used in this
380 study are listed in Table S1. *E. coli* strains were grown in Luria-Bertani medium (Oxoid) or on LB
381 agar (Oxoid). *S. aureus* strains were grown in Tryptic Soy Broth (TSB) or on Tryptic Soy Agar (TSA)
382 (both Oxoid). Ampicillin (100 µg/ml), chloramphenicol (10 µg/ml), or erythromycin (5 µg/ml) were
383 added when appropriate. Anhydrotetracycline (AHT) (Sigma-Aldrich) and Isopropyl β-D-1-
384 thiogalactopyranoside (IPTG) (Thermo Scientific) were used as inducers for protein expression.

385 **Construction of strains and plasmids.** All oligonucleotides used are listed in Table S1. *S. aureus*
386 8325-4Δ*sosA* is a clean deletion of *sosA* (SAOUHSC_01334) in strain 8325-4 obtained by allelic
387 replacement using the temperature-sensitive shuttle vector pIMAY (53). 1 kb regions up- and
388 downstream of *sosA* were PCR amplified (Phusion Hot Start II DNA Polymerase, Thermo Scientific)
389 using primer pairs Up-sosA_fw-KpnI/Up-sosA_rev and Dw-sosA_fw/Dw-sosA_rev-SacI,
390 respectively, and subsequently joined in a spliced overhang PCR using Up-sosA_fw-KpnI/Dw-
391 sosA_rev-SacI. The resulting deletion fragment was cloned into pIMAY via KpnI/SacI, generating
392 pIMAY-Δ*sosA*, purified from *E. coli* DC10B and transformed into *S. aureus* subsequently
393 maintained at 28°C. Chromosomal integration of the plasmid was performed at 37°C under

394 selective conditions (chloramphenicol) followed by passage at 28°C without antibiotic selection
395 and final plating on TSA containing 500 ng/ml of AHT for plasmid counterselection. Colonies were
396 replica-plated to select for sensitivity towards chloramphenicol and successful allelic exchange
397 were screened for by PCR amplification using primer pairs Ctrl_dsosA_F/Ctrl_dsosA_R positioned
398 outside *sosA* and Fwd_MCS/Rev_MCS targeting the vector, respectively. The allelic replacement
399 procedure was identical for *S. aureus* JE2 to create JE2Δ*sosA*.

400 The chromosomal transposon insertion mutation in *ctpA* conferring erythromycin resistance was
401 obtained from the Nebraska Transposon Mutant Library (NTML, NE847) (40) and was moved by
402 transduction (phage Φ11) to *S. aureus* JE2, JE2Δ*sosA*, S. *aureus* 8325-4 and 8325-4Δ*sosA*, resulting
403 in JE2-*ctpA*, JE2Δ*sosA*-*ctpA*, 8325-4-*ctpA* and 8325-4Δ*sosA*-*ctpA*, respectively. JE2-*ctpA*(−erm), an
404 erythromycin-sensitive derivative, was generated by elimination of the transposon-encoded *ermB*
405 in JE2-*ctpA* by allelic exchange using the pTnT vector using temperature-mediated chromosomal
406 integration and *secY*-mediated counterselection as described before (54).

407 All plasmid constructs mentioned below were cloned in E. coli IM08B (55) from where they were
408 transformed into *S. aureus* strains. For complementation of the *sosA* knockout, the *sosA* gene with
409 its native promoter was PCR amplified from strain 8325-4 using primers Up-sosA-promo_SalI and
410 Dw-sosA_EcoRI and cloned into designated restriction sites in plasmid pJC1112 (56). The resulting
411 plasmid (pJC1112-*sosA*) was transformed into the integration-proficient strain RN9011, creating
412 RN9011-*sosA*-compl. when selected with erythromycin. The chromosomally integrated plasmid
413 was transduced into 8325-4Δ*sosA*, resulting in 8325-4Δ*sosA*-compl. For *sosA* expression the *sosA*
414 gene including its predicted ribosomal binding site was cloned into the BglII and EcoRI sites of
415 pRAB12-*lacZ* (57) using primers Up-sosA_BglII/Dw-sosA_EcoRI, at the same time eliminating the

416 *lacZ* reporter gene. The resulting plasmid was called pSosA. Generation of plasmids encoding C-
417 terminally truncated variants of SosA was obtained by PCR amplification of DNA fragments using
418 Up-sosA_BglII and downstream primers Dw-sosA(d10)_EcoRI to Dw-sosA(d40)_EcoRI, all equipped
419 with premature stop codons. The PCR products were ligated into pRAB12-*lacZ* using BglII and
420 EcoRI cut sites to create pSosAd10, pSosAd20, pSosAd30 and pSosAd40. Single and double amino
421 acid substitutions (alanine) in the SosAd10 protein were obtained by cloning commercially
422 synthesized DNA fragments (Twist Bioscience) into pRAB12-*lacZ* using the same restriction sites.
423 The mutation at AA position 44 (D to A) was introduced to the full length SosA protein via
424 extension PCR by first using primers Up-sosA_BglII/SosA_R-long on the SosAd10(44A) template,
425 then using that product as template for amplification with primers Up-sosA_BglII/Dw-sosA_EcoRI
426 followed by cloning into pRAB12-*lacZ*, thereby generating pSosA(44A). Expression plasmids pPBP1,
427 pDivIC, pPBP3, pFtsL, pMurJ, and pCtpA were constructed by cloning the *pbpA*, *divIC*, *pbpC*, *ftsL*,
428 *murJ*, and *ctpA* genes behind the P_{spac} promoter in pSK9067 (58) using primer pairs pbpA_F-
429 SalI/pbpA_R-EcoRI, divIC-F_SalI/divIC-R_EcoRI, pbpC-F_SalI/pbpC-R_EcoRI, ftsL-F_SalI/ftsL-R_AatII,
430 murJ-F_SalI/murJ-R_AatII, and ctpA_F-SalI/ctpA_R-EcoRI, respectively. A plasmid for *pbpA**
431 expression was constructed by use of the same primer pair as for *pbpA* but using pMAD-PBP1*
432 (59) as a template. For membrane topology analysis using pKTop (39), *sosA*, *sosAd10*,
433 *sosAd10(44A)* and *sosAd40* were PCR amplified from respective expression constructs using
434 primer SosA_F-BamHI and primers SosA_R-KpnI, SosAd10_R-KpnI or SosAd40_R-KpnI, respectively,
435 and cloned in frame in front of the *phoA-lacZ* chimeric gene using BamHI/KpnI restriction sites.

436 In order to construct JE2 strains producing a fluorescent fusion of FtsZ, EzrA or GpsB in the
437 presence of the *sosA* expression plasmid, JE2 pSosA was transduced with a lysate from SH4665
438 (SH1000 pCQ11-FtsZ-eYFP), JGL227 (SH1000 *ezrA-gfp*+) or JGL228 (SH1000 *gpsB-gfp*+), resulting in

439 SJF4694 (JE2 pRAB12-*lacZ* pCQ11-FtsZ-eYFP), SJF4696 (JE2 pRAB12-*lacZ ezrA-gfp*+) and SJF4699
440 (JE2 pRAB12-*lacZ gpsB -gfp*+), respectively. Control strains SJF4693 (JE2 pRAB12-*lacZ* pCQ11-FtsZ-
441 eYFP), SJF4696 (JE2 pRAB12-*lacZ ezrA-gfp*+) and SJF4699 (JE2 pRAB12-*lacZ gpsB-gfp*+) were
442 constructed by a phage transduction of JE2 pRAB12-*lacZ* with lysates from SH4665 (SH1000
443 pCQ11-FtsZ-eYFP), JGL227 (SH1000 *ezrA-gfp*+) or JGL228 (SH1000 *gpsB-gfp*+), respectively. To
444 induce FtsZ-eYFP production in SJF4693 and SJF4694, cells were grown in the presence of 50 µM
445 IPTG.

446 In order to screen for interaction of SosA with cell-division/cell wall synthesis proteins of *S. aureus*,
447 *sosA* was amplified from *S. aureus* SH1000 genomic DNA using primers ALB133 and ALB134, and
448 ligated into pUT18C using BamHI/EcoRI cut sites, resulting in pT18-SosA. T18 fusions with SosAd10
449 and SosAd40 were generated by combining ALB133 with respective truncation primers (Dw-
450 sosA(d10)_EcoRI and Dw-sosA(d40)_EcoRI). The pT18-SosA(44A) plasmid was obtained as above
451 but by use of pSosA(44A) as PCR amplification template. All fusion constructs to T25 and control
452 vectors were generated previously (43, 60-62, Table S1).

453 **Determination of OD_{600} and CFU after MMC treatment.** Strains were grown overnight on TSA
454 plates and used for inoculating TSB and allowed to grow to OD_{600} = 0.05 when Mitomycin C (MMC
455 from *Streptomyces caespitosus*, Sigma-Aldrich) was added. Cell density was monitored by OD_{600}
456 measurements at intervals onwards and samples were withdrawn to determine culture colony
457 forming units by serial dilution in 0.9% w/v NaCl and plating on TSA.

458 **Flow cytometry.** Cell size distributions of cultures were arbitrarily quantified by flow cytometry
459 using the forward scatter signal (FSC-A) acquired on a BD Accuri™ C6 flow cytometer (BD
460 Biosciences). Cell samples were diluted in 0.9% w/v NaCl to an approximate density of 10^6 cells/ml

461 and sonicated briefly to allow acquisition of scatter signal from single cells predominantly.
462 Sonication was performed with a Bandelin sonopuls HD2070/UW2070 apparatus (Bandelin
463 electronics, Germany) fitted with the MS 73 probe. Ten pulses of 500 msec were given at 50%
464 power. All flow cytometry experiments were independently repeated at least twice with similar
465 results.

466 **Plating assays.** Spot dilution was used to evaluate plating efficiency of strains carrying various
467 plasmid constructs. Strains were grown exponentially until an approximate OD_{600} of 0.5 under
468 plasmid selective conditions. Strains were then ten-fold serially diluted in 0.9% w/v NaCl and
469 positioned as 10 µl spots on TSA containing selective antibiotics with/without inducer at indicated
470 concentrations and incubated at 37°C overnight. All spot plating assays were independently
471 repeated with similar results.

472 **Labelling *S. aureus* with HADA**

473 Cells grown to mid-exponential phase (OD_{600} ~ 0.5) were incubated with 500 µM HADA at 37°C for
474 5 min. Cells were then washed by centrifugation and resuspension in PBS.

475 **Labelling *S. aureus* with NHS ester**

476 Labelling with NHS ester was performed as described before (34). Briefly, cells grown to mid-
477 exponential phase (OD_{600} ~0.5) were collected by centrifugation and growth medium was
478 discarded. Cells were resuspended in PBS containing 8 µg ml^{-1} Alexa Fluor 647 NHS ester
479 (Invitrogen) and incubated at room temperature for 5 min. Cells were washed by centrifugation
480 and resuspension in PBS.

481 **Fixing**

482 Cells were fixed by incubation in 4% (w/v) paraformaldehyde at room temperature for 30 min.

483 **Widefield Epifluorescence Microscopy**

484 Fixed cells were dried onto a poly-L-Lysine coated slide and mounted in PBS. Imaging was
485 performed using either a Nikon Ti Inverted microscope fitted with a Lumencor Spectra X light
486 engine or a v4 DeltaVision OMX 3D-SIM system (Applied Precision, GE Healthcare, Issaquah, USA).

487 **3D Structured Illumination Microscopy**

488 A high precision cover slip (High-precision, No.1.5H, 22x22mm, 170±5 µm, Marienfeld) was
489 cleaned by sonicating in 1 M KOH for 15 min at room temperature. The coverslip was washed with
490 water and incubated in 0.01% (w/v) poly-L-lysine solution (Sigma) for 30 min at room
491 temperature. The coverslip was rinsed with water and dried with nitrogen. Fixed cells were dried
492 onto the poly-L-Lysine coated cover slip and mounted on a slide with SlowFade Diamond
493 (Invitrogen). 3D SIM visualisation was performed using a v4 DeltaVision OMX 3D-SIM system
494 (Applied Precision, GE Healthcare, Issaquah, USA) equipped with a Plan Apo 60x, 1.42 NA oil
495 objective, using 1.514 immersion oil, a 642 nm laser and a standard excitation/emission filter set
496 (683/40). For each z-section, a sample was imaged in 5 phase shifts and 3 angles. The z-sections
497 were 0.125 nm in depth. Raw data were reconstructed with the Softworx software (GE
498 Healthcare) using OTFs optimized for the specific wavelength and oil used.

499 **Time-lapse microscopy.** Strains were grown overnight in TSB medium at 37°C, then diluted 100
500 times in fresh TSB and grown until OD = 0.1. Cells were washed once with fresh TSB and spotted
501 onto TSB-acrylamide (10%) pads previously incubated for 2h in TSB medium supplemented, when
502 appropriate, with 0.04 µg/mL mitomycin C (MMC) or 200 ng/mL anhydrotetracycline (AHT). Pads
503 were placed into a Gene frame (Thermo Fisher Scientific) and sealed with a cover glass. Phase-

504 contrast images were acquired on a DV Elite microscope (GE healthcare) equipped with a sCMOS
505 (PCO) camera and a 100x oil-immersion objective. Images were acquired with 200 ms exposure
506 time every 4 minutes for at least 6 h at 37°C using Softworx (Applied Precision) software. Images
507 were analyzed using Fiji (http://fiji.sc).

508 **Western blot analysis.** Purified rabbit anti-SosA antibody was obtained via GenScript Biotech
509 (Netherlands). A custom peptide, CEHKDPTNNSEQRDGA, comprising AAs 57-70 of SosA was used
510 for immunization. Bacterial cells were pelleted and frozen immediately at -80°C before being
511 resuspended in PBS containing cOmplete™ Mini Protease Inhibitor Cocktail (Sigma-Aldrich) and
512 lysed by bead-beating (Fastprep-24™, MP Biomedicals). The protein concentration of the lysates
513 was measured using the Qubit™ Protein Assay Kit (ThermoFisher Scientific) and samples were
514 normalized to equal amounts of protein, 20 µg of total protein was separated on NuPAGE® 4-12%
515 Bis-Tris gels using MES buffer and the XCell sure-lock mini-cell system (ThermoFisher Scientific),
516 transferred to a polyvinylidene difluoride membrane(PVDF) and probed with primary antibody
517 diluted 1:1000. Bound antibody was detected with the WesternBreeze® Chemiluminescent Kit,
518 anti-rabbit according to the instructions from the manufacturer (ThermoFisher Scientific). All
519 western blots were independently repeated with similar results. Uncropped versions of blots are
520 displayed in Fig S6.

521 **Bacterial two-hybrid assay.** Interactions between SosA and proteins involved in cell division and
522 cell wall synthesis of *S. aureus* were tested using *E.coli* BTH101 (Δ*cyaA*) cotransformed with pT18-
523 SosA and a plasmid carrying a fusion of T25 with a cell-division or cell wall synthesis protein on
524 minimal medium as previously described (43). Mutant and truncated variants of SosA were tested

525 specifically for interaction with PBP1 and DivIC in comparison to the interaction observed with the
526 wildtype protein.

527 **Acknowledgements**

528 This work was supported by grants from the Danish Council for Independent Research –
529 Technology and Production (1337-00129 and 1335-00772) to M.S.B., by the Danish National
530 Research Foundation (DNRF120) to H.I., and by the Medical Research Council (MR/K015753/1 to
531 the Wolfson Light Microscopy Facility at the University of Sheffield and MR/N002679/1). We
532 would like to thank Prof Simon Jones (University of Sheffield) for the HADA dye.

533 M.S.B., K.W., P.K., M.T.C., S.J.F., and H.I. conceived and designed the study. Experiments were
534 performed by M.S.B., K.W., C.G., and A.L.B. M.S.B. K.W., C.G., G.L., D.F., J.-W.V., S.J.F., and H.I.
535 contributed to analysis of data and drafting of the manuscript. All authors read and approved the
536 final manuscript.

537

538 **References**

539 1. Sass P, Brötz-Oesterhelt H. 2013. Bacterial cell division as a target for new antibiotics. Curr
540 Opin Microbiol 16:522-530.
541 2. Lock RL, Harry EJ. 2008. Cell-division inhibitors: new insights for future antibiotics. Nat Rev
542 Drug Discov 7:324-338.
543 3. Robinson A, Causer RJ, Dixon NE. 2012. Architecture and conservation of the bacterial DNA
544 replication machinery, an underexploited drug target. Curr Drug Targets 13:352-372.

545 4. Adams DW, Errington J. 2009. Bacterial cell division: assembly, maintenance and
546 disassembly of the Z ring. Nat Rev Microbiol 7:642-653.
547 5. Baharoglu Z, Mazel D. 2014. SOS, the formidable strategy of bacteria against aggressions.
548 FEMS Microbiol Rev 38:1126-1145.
549 6. Kreuzer KN. 2013. DNA damage responses in prokaryotes: regulating gene expression,
550 modulating growth patterns, and manipulating replication forks. Cold Spring Harb Perspect
551 Biol 5:a012674.
552 7. Kelley WL. 2006. Lex marks the spot: the virulent side of SOS and a closer look at the LexA
553 regulon. Mol Microbiol 62:1228-1238.
554 8. Huisman O, D'Ari R. 1981. An inducible DNA replication-cell division coupling mechanism in
555 E. coli. Nature 290:797-799.
556 9. Huisman O, D'Ari R, Gottesman S. 1984. Cell-division control in Escherichia coli: specific
557 induction of the SOS function SfiA protein is sufficient to block septation. Proc Natl Acad Sci
558 U S A 81:4490-4494.
559 10. Jones C, Holland IB. 1985. Role of the SulB (FtsZ) protein in division inhibition during the
560 SOS response in Escherichia coli: FtsZ stabilizes the inhibitor SulA in maxicells. Proc Natl
561 Acad Sci U S A 82:6045-6049.
562 11. Higashitani A, Higashitani N, Horiuchi K. 1995. A cell division inhibitor SulA of Escherichia
563 coli directly interacts with FtsZ through GTP hydrolysis. Biochem Biophys Res Commun
564 209:198-204.
565 12. Mukherjee A, Cao C, Lutkenhaus J. 1998. Inhibition of FtsZ polymerization by SulA, an
566 inhibitor of septation in Escherichia coli. Proc Natl Acad Sci U S A 95:2885-2890.

567 13. Cordell SC, Robinson E J, Lowe J. 2003. Crystal structure of the SOS cell division inhibitor
568 SulA and in complex with FtsZ. Proc Natl Acad Sci U S A 100:7889-7894.
569 14. Schoemaker JM, Gayda RC, Markovitz A. 1984. Regulation of cell division in Escherichia coli:
570 SOS induction and cellular location of the sulA protein, a key to lon-associated
571 filamentation and death. J Bacteriol 158:551-561.
572 15. Mizusawa S, Gottesman S. 1983. Protein degradation in Escherichia coli: the lon gene
573 controls the stability of sulA protein. Proc Natl Acad Sci U S A 80:358-362.
574 16. Modell JW, Hopkins AC, Laub MT. 2011. A DNA damage checkpoint in Caulobacter
575 crescentus inhibits cell division through a direct interaction with FtsW. Genes Dev 25:1328-
576 1343.
577 17. Modell JW, Kambara TK, Perchuk BS, Laub MT. 2014. A DNA damage-induced, SOS-
578 independent checkpoint regulates cell division in Caulobacter crescentus. PLoS Biol
579 12:e1001977.
580 18. Tzagoloff H, Novick R. 1977. Geometry of cell division in Staphylococcus aureus. J Bacteriol
581 129:343-350.
582 19. Turner RD, Ratcliffe EC, Wheeler R, Golestanian R, Hobbs JK, Foster SJ. 2010. Peptidoglycan
583 architecture can specify division planes in Staphylococcus aureus. Nat Commun 1:26.
584 20. Pinho MG, Kjos M, Veening JW. 2013. How to get (a)round: mechanisms controlling growth
585 and division of coccoid bacteria. Nat Rev Microbiol 11:601-614.
586 21. Cirz RT, Jones MB, Gingles NA, Minogue TD, Jarrahi B, Peterson SN, Romesberg FE. 2007.
587 Complete and SOS-mediated response of Staphylococcus aureus to the antibiotic
588 ciprofloxacin. J Bacteriol 189:531-539.

589 22. Anderson KL, Roberts C, Disz T, Vonstein V, Hwang K, Overbeek R, Olson PD, Projan SJ,
590 Dunman PM. 2006. Characterization of the Staphylococcus aureus heat shock, cold shock,
591 stringent, and SOS responses and their effects on log-phase mRNA turnover. J Bacteriol
592 188:6739-6756.
593 23. Cohn MT, Kjelgaard P, Frees D, Penadés JR, Ingmer H. 2011. Clp-dependent proteolysis of
594 the LexA N-terminal domain in Staphylococcus aureus. Microbiology 157:677-684.
595 24. Mesak LR, Miao V, Davies J. 2008. Effects of subinhibitory concentrations of antibiotics on
596 SOS and DNA repair gene expression in Staphylococcus aureus. Antimicrob Agents
597 Chemother 52:3394-3397.
598 25. Kawai Y, Moriya S, Ogasawara N. 2003. Identification of a protein, YneA, responsible for
599 cell division suppression during the SOS response in Bacillus subtilis. Mol Microbiol 47:
600 1113-1122.
601 26. Buchholz M, Nahrstedt H, Pillukat MH, Deppe V, Meinhardt F. 2013. yneA mRNA instability
602 is involved in temporary inhibition of cell division during the SOS response of Bacillus
603 megaterium. Microbiology 159:1564-1574.
604 27. van der Veen S, Hain T, Wouters JA, Hossain H, de Vos WM, Abee T, Chakraborty T Wells-
605 Bennik MH. 2007. The heat-shock response of Listeria monocytogenes comprises genes
606 involved in heat shock, cell division, cell wall synthesis, and the SOS response. Microbiology
607 153:3593-3607.
608 28. van der Veen S, van Schalkwijk S, Molenaar D, de Vos WM, Abee T, Wells-Bennik MH. 2010.
609 The SOS response of Listeria monocytogenes is involved in stress resistance and
610 mutagenesis. Microbiology 156:374-384.

611 29. Chauhan A, Lofton H, Maloney E, Moore J, Fol M, Madiraju MV, Rajagopalan M. 2006.
612 Interference of Mycobacterium tuberculosis cell division by Rv2719c, a cell wall hydrolase.
613 Mol Microbiol 62:132-147.
614 30. Ogino H, Teramoto H, Inui M, Yukawa H. 2008. DivS, a novel SOS-inducible cell-division
615 suppressor in Corynebacterium glutamicum. Mol Microbiol 67:597-608.
616 31. Buist G, Steen A, Kok J, Kuipers OP. 2008. LysM, a widely distributed protein motif for
617 binding to (peptido)glycans. Mol Microbiol 68:838-847.
618 32. Mesnage S, Dellarole M, Baxter NJ, Rouget JB, Dimitrov JD, Wang N, Fujimoto Y, Hounslow
619 AM, Lacroix-Desmazes S, Fukase K, Foster SJ, Williamson MP. 2014. Molecular basis for
620 bacterial peptidoglycan recognition by LysM domains. Nat Commun 5:4269.
621 33. Monteiro JM, Fernandes PB, Vaz F, Pereira AR, Tavares AC, Ferreira MT, Pereira PM, Veiga
622 H, Kuru E, VanNieuwenhze MS, Brun YV, Filipe SR, Pinho MG. 2015. Cell shape dynamics
623 during the staphylococcal cell cycle. Nat Commun 6:8055.
624 34. Lund VA, Wacnik K, Turner RD, Cotterell BE, Walther CG, Fenn SJ, Grein F, Wollman AJ,
625 Leake MC, Olivier N, Cadby A, Mesnage S, Jones S, Foster SJ. 2018. Molecular coordination
626 of Staphylococcus aureus cell division. Elife 7:e32057.
627 35. Monteiro JM, Pereira AR, Reichmann NT, Saraiva BM, Fernandes PB, Veiga H, Tavares AC,
628 Santos M, Ferreira MT, Macário V, VanNieuwenhze MS, Filipe SR, Pinho MG. 2018.
629 Peptidoglycan synthesis drives an FtsZ-treadmilling-independent step of cytokinesis.
630 Nature 554:528-532.
631 36. Vadrevu IS, Lofton H, Sarva K, Blasczyk E, Plocinska R, Chinnaswamy J, Madiraju M,
632 Rajagopalan M. 2011. ChiZ levels modulate cell division process in mycobacteria.
633 Tuberculosis (Edinb) 91:S128-135.

634 37. Mo AH, Burkholder WF. 2010. YneA, an SOS-induced inhibitor of cell division in Bacillus
635 subtilis, is regulated posttranslationally and requires the transmembrane region for
636 activity. J Bacteriol 192:3159-3173.
637 38. Tsirigos KD, Peters C, Shu N, Käll L, Elofsson A. 2015. The TOPCONS web server for
638 consensus prediction of membrane protein topology and signal peptides. Nucleic Acids Res
639 43:W401-7.
640 39. Karimova G, Ladant D. 2017. Defining Membrane Protein Topology Using pho-lac Reporter
641 Fusions. Methods Mol Biol 1615:129-142.
642 40. Fey PD, Endres JL, Yajjala VK, Widhelm TJ, Boissy RJ, Bose JL, Bayles KW. 2013. A genetic
643 resource for rapid and comprehensive phenotype screening of nonessential
644 Staphylococcus aureus genes. MBio 4:e00537-12.
645 41. Carroll RK, Rivera FE, Cavaco CK, Johnson GM, Martin D, Shaw LN. 2014. The lone S41
646 family C-terminal processing protease in Staphylococcus aureus is localized to the cell wall
647 and contributes to virulence. Microbiology 160:1737-1748.
648 42. Burby PE, Simmons ZW, Schroeder JW, Simmons LA. 2018. Discovery of a dual protease
649 mechanism that promotes DNA damage checkpoint recovery. PLoS Genet 14:e1007512.
650 43. Steele VR, Bottomley AL, Garcia-Lara J, Kasturiarachchi J, Foster SJ. 2011. Multiple essential
651 roles for EzrA in cell division of Staphylococcus aureus. Mol Microbiol 80:542-555.
652 44. Bottomley AL, Kabli AF, Hurd AF, Turner RD, Garcia-Lara J, Foster SJ. 2014. Staphylococcus
653 aureus DivIB is a peptidoglycan-binding protein that is required for a morphological
654 checkpoint in cell division. Mol Microbiol 94:1041-1064.
655 45. Gamba P, Veening JW, Saunders NJ, Hamoen LW, Daniel RA. 2009. Two-step assembly
656 dynamics of the Bacillus subtilis divisome. J Bacteriol 191:4186-4194.

657 46. Kawai Y, Ogasawara N. 2006. Bacillus subtilis EzrA and FtsL synergistically regulate FtsZ ring
658 dynamics during cell division. Microbiology 152:1129-1141.
659 47. Pereira SF, Henriques AO, Pinho MG, de Lencastre H, Tomasz A. 2007. Role of PBP1 in cell
660 division of Staphylococcus aureus. J Bacteriol 189:3525-3531.
661 48. Pereira SF, Henriques AO, Pinho MG, de Lencastre H, Tomasz A. 2009. Evidence for a dual
662 role of PBP1 in the cell division and cell separation of Staphylococcus aureus. Mol
663 Microbiol 72:895-904.
664 49. den Blaauwen T, Hamoen LW, Levin PA. 2017. The divisome at 25: the road ahead. Curr
665 Opin Microbiol 36:85-94.
666 50. Daniel RA, Noirot-Gros MF, Noirot P, Errington J. 2006. Multiple interactions between the
667 transmembrane division proteins of Bacillus subtilis and the role of FtsL instability in
668 divisome assembly. J Bacteriol 188:7396-7404.
669 51. Pinho MG, de Lencastre H, Tomasz A. 2000. Cloning, characterization, and inactivation of
670 the gene pbpC, encoding penicillin-binding protein 3 of Staphylococcus aureus. J Bacteriol
671 182:1074-1079.
672 52. Daniel RA, Harry EJ, Katis VL, Wake RG, Errington J. 1998. Characterization of the essential
673 cell division gene ftsL(yIID) of Bacillus subtilis and its role in the assembly of the division
674 apparatus. Mol Microbiol 29:593-604.
675 53. Monk IR, Shah IM, Xu M, Tan MW, Foster TJ. 2012. Transforming the untransformable:
676 application of direct transformation to manipulate genetically Staphylococcus aureus and
677 Staphylococcus epidermidis. MBio 3:e00277-11.
678 54. Bose JL, Fey PD, Bayles KW. 2013. Genetic tools to enhance the study of gene function and
679 regulation in Staphylococcus aureus. Appl Environ Microbiol 79:2218-2224.

680 55. Monk IR, Tree JJ, Howden BP, Stinear TP, Foster TJ. 2015. Complete Bypass of Restriction
681 Systems for Major Staphylococcus aureus Lineages. MBio 6:e00308-15.
682 56. Chen J, Yoong P, Ram G, Torres VJ, Novick RP. 2014. Single-copy vectors for integration at
683 the SaPI1 attachment site for Staphylococcus aureus. Plasmid 76:1-7.
684 57. Helle L, Kull M, Mayer S, Marincola G, Zelder ME, Goerke C, Wolz C, Bertram R. 2011.
685 Vectors for improved Tet repressor-dependent gradual gene induction or silencing in
686 Staphylococcus aureus. Microbiology 157:3314-3323.
687 58. Brzoska AJ, Firth N. 2013. Two-plasmid vector system for independently controlled
688 expression of green and red fluorescent fusion proteins in Staphylococcus aureus. Appl
689 Environ Microbiol 79:3133-3136.
690 59. Wacnik K. 2016. Dissecting cell division in the human pathogen Staphylococcus aureus.
691 PhD Thesis. University of Sheffield.
692 60. Karimova G, Pidoux J, Ullmann A, Ladant D. 1998. A bacterial two-hybrid system based on a
693 reconstituted signal transduction pathway. Proc Natl Acad Sci U S A 95:5752-5756.
694 61. Claessen D, Emmins R, Hamoen LW, Daniel RA, Errington J, Edwards DH. 2008. Control of
695 the cell elongation-division cycle by shuttling of PBP1 protein in Bacillus subtilis. Mol
696 Microbiol 68:1029-1046.
697 62. Bottomley AL, Liew ATF, Kusuma KD, Peterson E, Seidel L, Foster SJ, Harry EJ. 2017.
698 Coordination of Chromosome Segregation and Cell Division in Staphylococcus aureus.
699 Front Microbiol 8:1575.

700

701

Figures

Figure 1

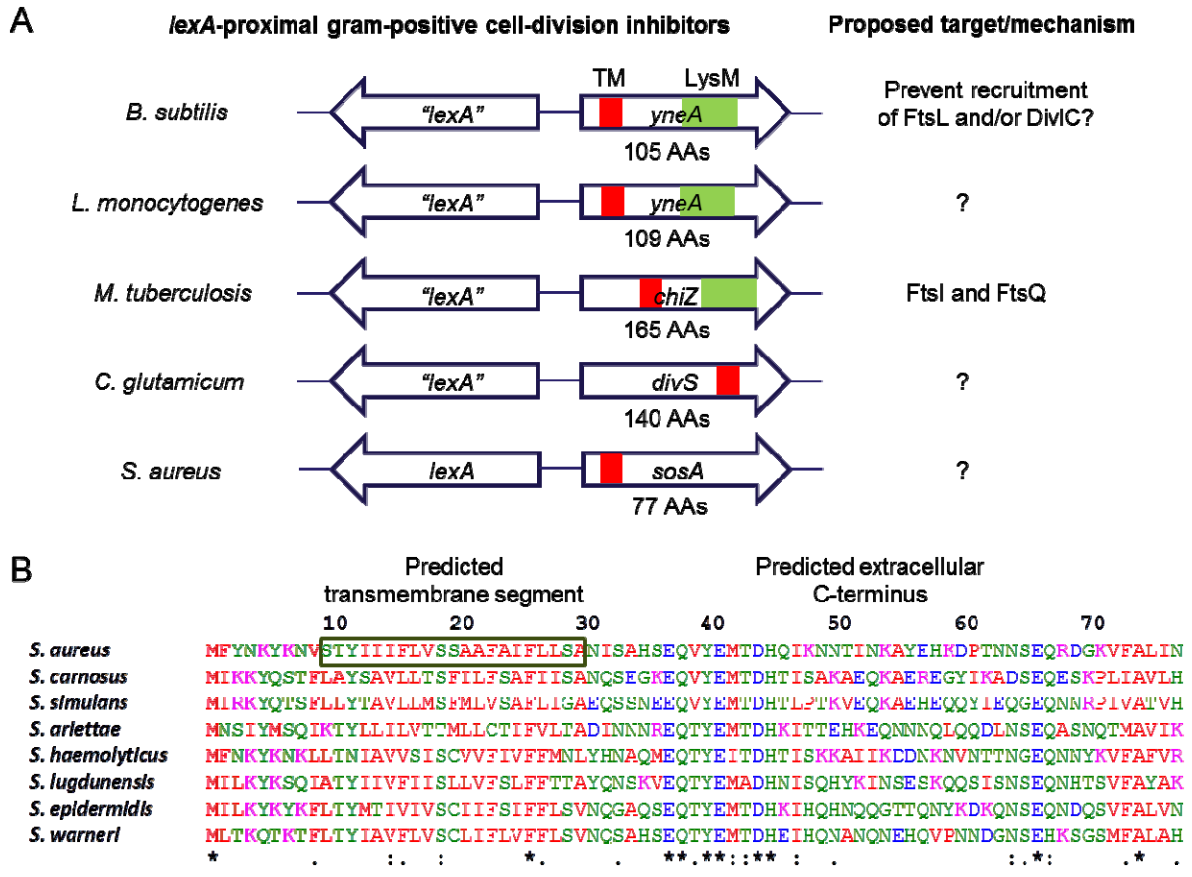

Fig 1 Gram-positive SOS-controlled cell-division inhibitors. (A) Schematic representation of genes encoding characterized gram-positive SOS-regulated cell-division inhibitors (not drawn to scale) including the uncharacterized *sosA* from *S. aureus*. Despite considerable sequence divergence, these genes are commonly chromosomally co-localized with *lexA* homologous genes. The cell-division inhibitors carry a single transmembrane domain (TM), and several proteins have an additional LysM domain. (B) Alignment (CLUSTAL O[1.2.4]) of SosA sequences deduced from open reading frames next to *lexA* in *S. aureus* strain 8325-4 (YP_499864) and seven *Staphylococcus* species: *S. carnosus* (CAL27889), *S. simulans* (AMG96201), *S. arlettae* (EJY94737), *S. haemolyticus*

713 (YP_253482), *S. lugdunensis* (YP_003471776), *S. epidermidis* (YP_188489), and *S. warneri*

714 (EEQ79882). The proteins are 77 amino acids long and are characterized by a predicted

715 transmembrane segment at AAs 10-30 (for *S. aureus* SosA) and a predicted extracellular C-

716 terminal (TOPCONS [37]) with considerable sequence conservation at the membrane-proximal

717 portion ("*" indicates fully conserved residues, ":" indicates conservation of residues with highly

718 similar properties).

719

720 **Figure 2**

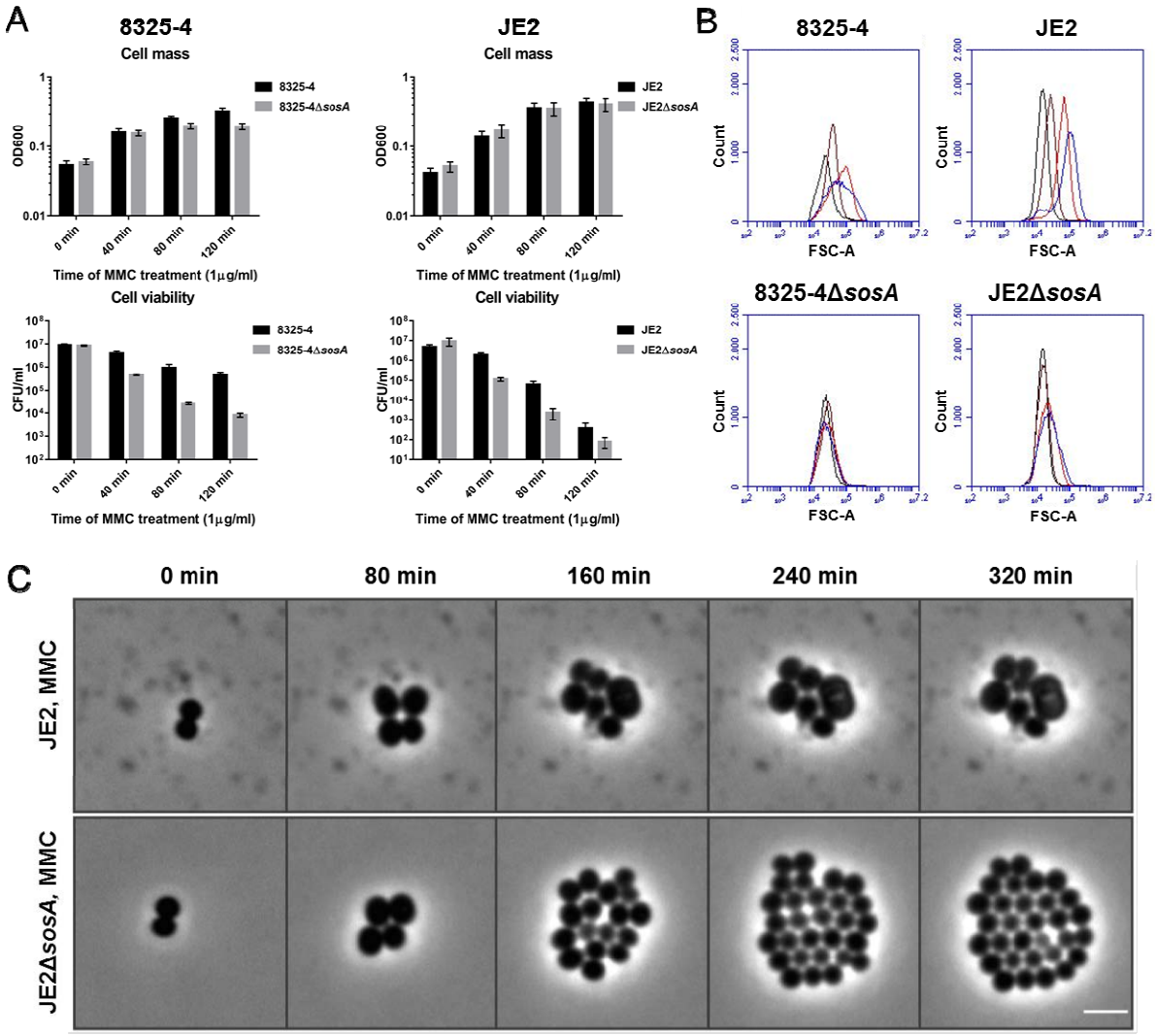

721

722

723 **Fig 2** SosA supports survival of *S. aureus* subjected to lethal DNA damage and is involved in

724 bacterial swelling. (A) Culture optical density at 600 nm and cell viability of *S. aureus* strains 8325-

725 4 and JE2 in comparison with their respective *ΔsosA* mutants upon challenge with a lethal dose of

726 mitomycin C (MMC, 1 µg/ml) for two hours. Error bars represent the standard deviation from

727 three biological replicates. (B) Cell size of 8325-4 and JE2 wildtype and *ΔsosA* mutants exposed to

728 mitomycin C estimated by flow cytometry (FSC-A). Cells were grown exponentially prior to MMC

729 addition at an OD_{600} of 0.05. Samples were taken after 0 (black), 40 (brown), 80 (red), and 120

730 (blue) minutes of incubation with MMC. (C) Effect of MMC treatment (0.04 µg/mL) on cell shape

731 and cell number of JE2 wildtype and JE2Δ*sosA* as visualized by time-lapse phase-contrast

732 microscopy. Scale bar represents 2 µm.

733

734 **Figure 3**

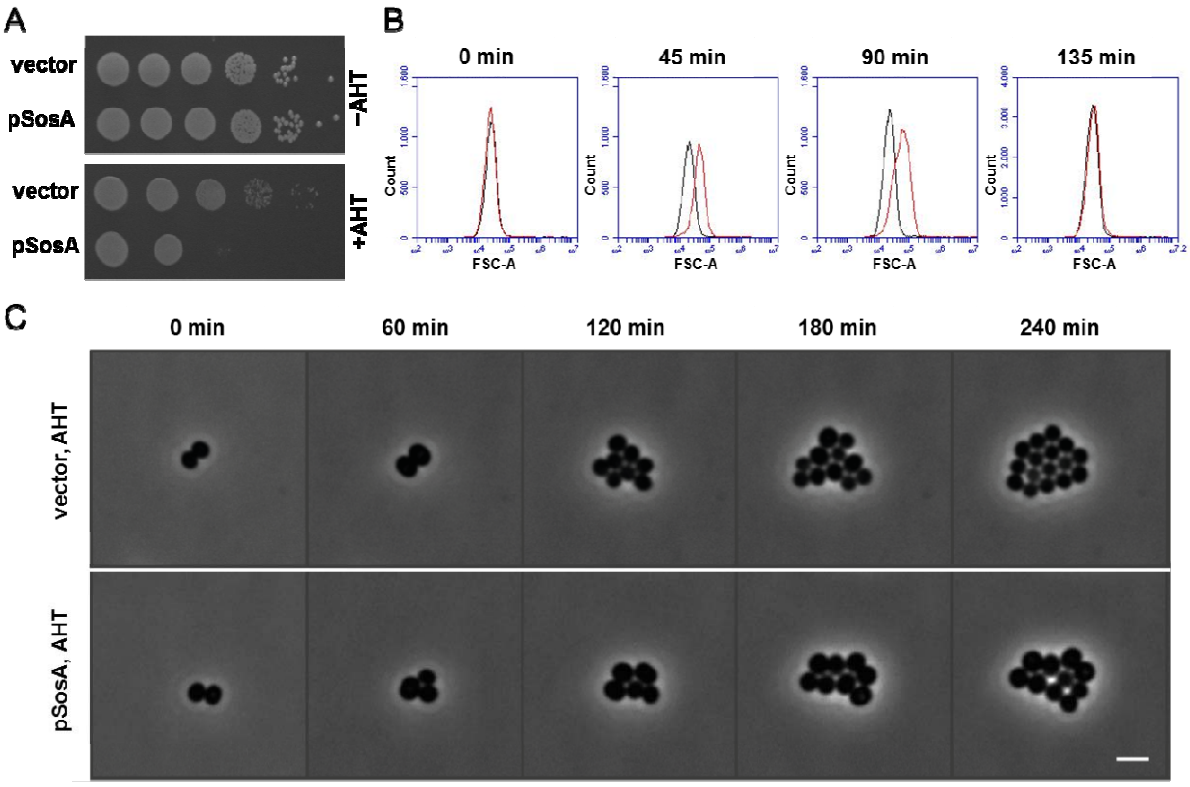

735

736

737 **Fig 3** Expression of *sosA* alone interferes with *S. aureus* growth. (A) The effect of a controlled

738 expression of *sosA* on the ability to form colonies was assessed in *S. aureus* RN4220. Strains

739 carrying either the vector control (vector) or *sosA* under an anhydrotetracycline (AHT)-inducible

740 promoter (pSosA) were grown exponentially to an OD_{600} of 0.5, serially 10-fold diluted, and plated

741 on TSA plates in the presence or absence of TSA+300 ng/ml of AHT. The plates were incubated

742 overnight at 37°C and imaged. (B) Evaluation of cell size distribution by flow cytometry (FSC-A) of

743 *S. aureus* RN4220 containing the control vector (black) or pSosA (red). Cells were grown

744 exponentially prior to induction with 100 ng/ml of AHT. At the indicated time points, the cells

745 were collected and analyzed by flow cytometry. (C) Visualization of cell size increase and reduction

746 of cell number of JE2/pRAB12-*lacZ* (control) and JE2/pRAB12-*sosA* in the presence of 200 ng/mL of

747 AHT by time-lapse phase-contrast microscopy at 37°C. Scale bar represents 2 µm.

748

749 **Figure 4**

750

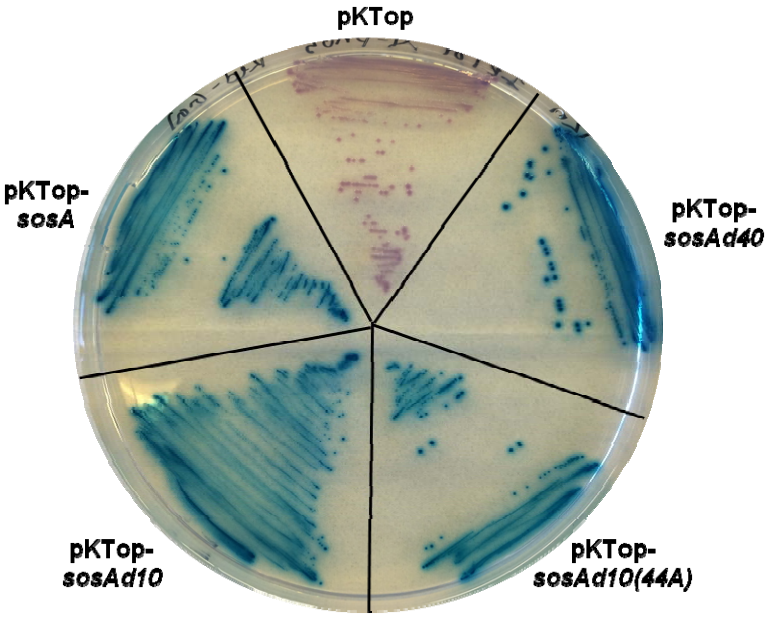

751

752 **Fig 4** Evaluation of membrane localization of SosA and truncated variants SosAd10, SosAd10(44A),

753 and SosAd40 by in frame fusion at the C-terminus to PhoA-LacZ in pKTop (the truncated variants

754 are explained in Fig. 5 and Fig. 6). *E. coli* IM08B cells carrying the constructs were streaked on a

755 dual indicator plate containing LB agar plus 50 µg/ml of kanamycin, 1 mM IPTG, 5-bromo-4-

756 chloro-3-indolyl phosphate disodium salt (80 µg/ml) and 6-Chloro-3-indolyl-β-D-galactopyranoside

757 (100 µg/ml). Cytoplasmic localization of the PhoA-LacZ chimera is indicated by red/rose color

758 development whereas translocation across the membrane is indicated by blue color development.

759

760

761 **Figure 5**

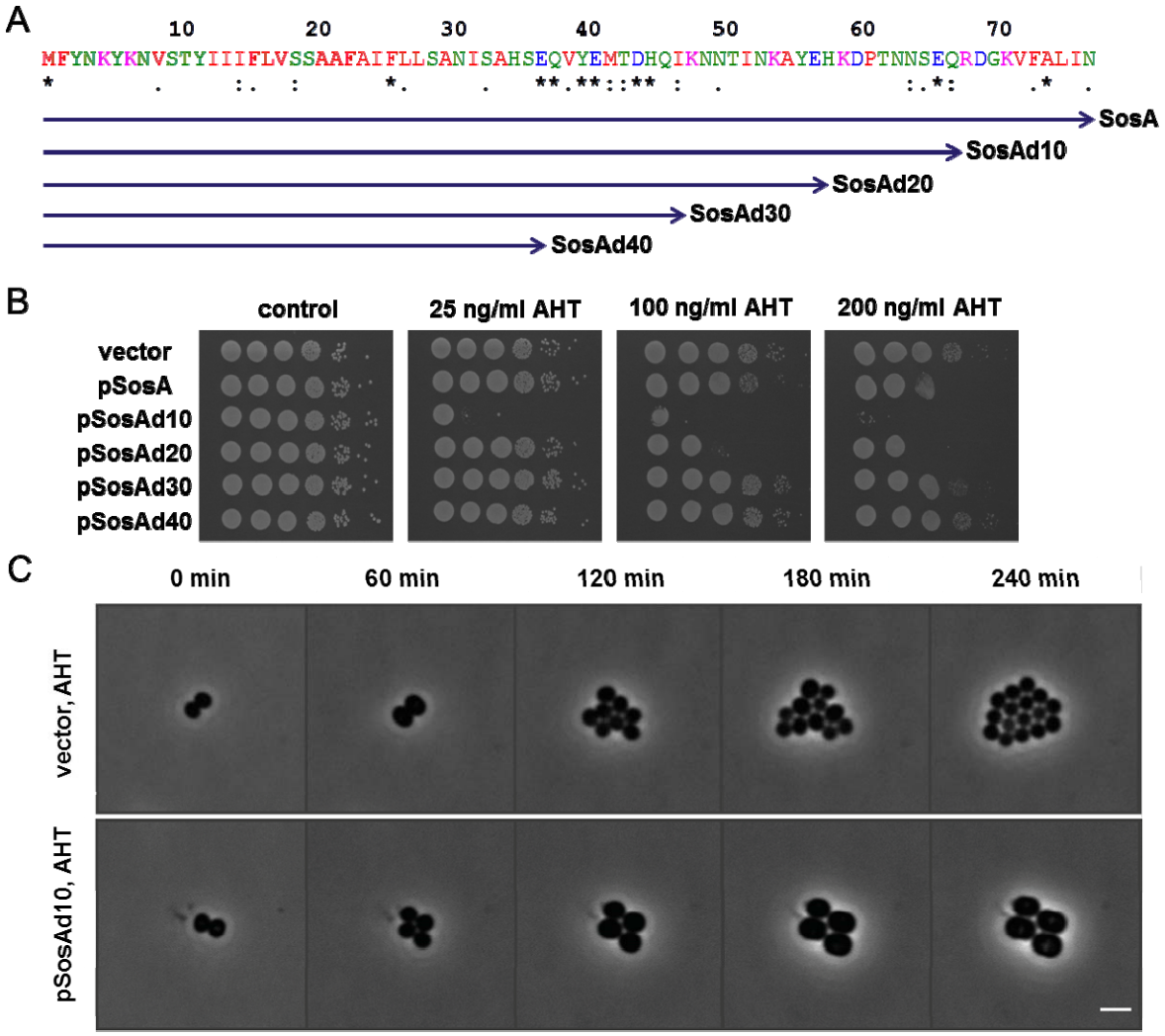

762

763

764 **Fig 5** The effect of C-terminal truncations of SosA on the inhibitory activity of the protein. (A)

765 Schematic representation of the different truncated SosA constructs. Full-length SosA is a 77-

766 amino-acid peptide. SosAd10 lacks the extreme C-terminal 10 amino acids, while SosAd40 is SosA

767 truncated of almost its entire extracellular C-terminal part. Indicated conserved residues (*****)

768 originate from the alignment in Figure 1. (B) Activity of the constructs was assessed in *S. aureus*

769 RN4220 and compared to the vector control (vector). Cells were grown exponentially to an OD_{600}

770 of 0.5, serially 10-fold diluted, and plated on TSA (control) or TSA plus inducer (AHT) at indicated

771 increasing concentrations followed by incubation overnight at 37°C. (C) Visualization of the drastic

772 cell size increase and the reduction in cell number of JE2/pRAB12-*lacZ* (control) and JE2/pRAB12-

773 *sosAd10* in presence of 200 ng/mL of AHT by time-lapse phase-contrast microscopy at 37°C. Scale

774 bar represents 2 µm.

775

776 **Figure 6**

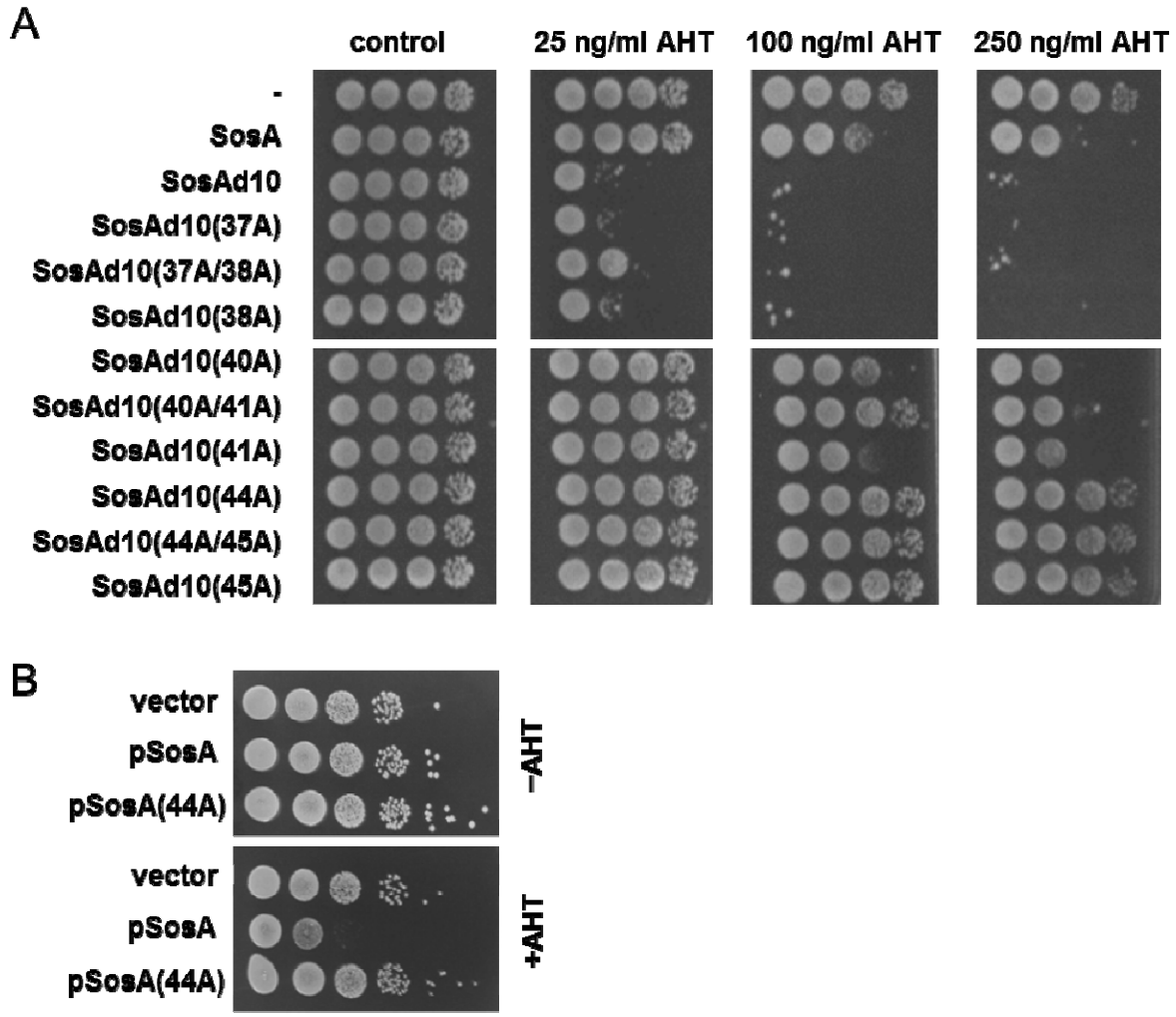

777

778 **Fig 6** (A) Assessment of the activity of SosAd10 variants with point mutations (alanine
779 substitutions) at conserved residues (37/38, 40/41, and 44/45) within the C-terminal part. Activity
780 of the constructs was assessed in *S. aureus* JE2 and compared to the vector control (-), SosA, and
781 SosAd10. Cells were grown exponentially to an OD_{600} of 0.5, serially 10-fold diluted, and plated on
782 TSA (control) or TSA plus inducer (AHT) at increasing concentrations followed by incubation
783 overnight at 37°C. (B) Comparison of the activity of the point mutation protein SosA(44A) with
784 wildtype SosA in *S. aureus* JE2. Cells were grown as above and plated on TSA or TSA plus 200 ng/ml
785 AHT.

786

787

788 **Figure 7**

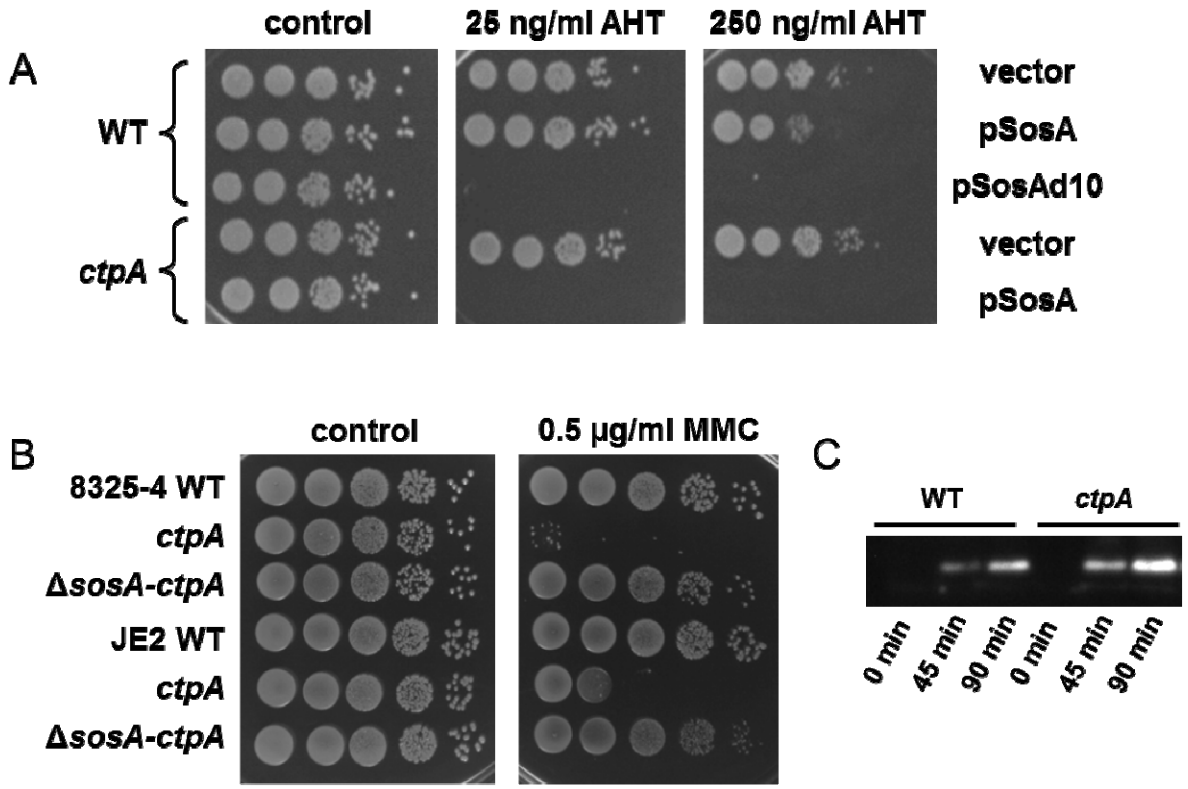

789

790

791 **Fig 7** CtpA is a possible negative regulator of SosA. (A) Hypersusceptibility of an *S. aureus* JE2 *ctpA*

792 mutant to SosA-mediated growth inhibition. Expression of *sosA* (pSosA) in wildtype *S. aureus* JE2

793 (WT) and the corresponding JE2-*ctpA* mutant (*ctpA*) were compared and referenced to the vector

794 control (vector) and expression of the hyperactive SosAd10 variant (pSosAd10) in the wildtype.

795 Cells were grown exponentially to an OD_{600} of 0.5, serially 10-fold diluted, and plated on TSA

796 (Control) or TSA plus inducer (AHT) at indicated concentrations. The plates were incubated

797 overnight at 37°C and imaged. (B) Assessment of mitomycin C susceptibility of a *ctpA* mutant by

798 comparison of plating efficiency of *S. aureus* 8325-4 and JE2 wildtype, *ctpA*, and Δ*sosA-ctpA* in

799 presence of 0.5 µg/ml MMC. Cells were grown exponentially to an OD_{600} of 0.5 and serially 10-fold

800 diluted before plating and incubation at 37°C overnight. (C) Western blot of accumulated SosA in

801 *S. aureus* 8325-4 wildtype (WT) and the *ctpA* mutant at indicated time points after the addition of

802 1 µg/ml of MMC to exponentially growing cells.

803

804 **Figure 8**

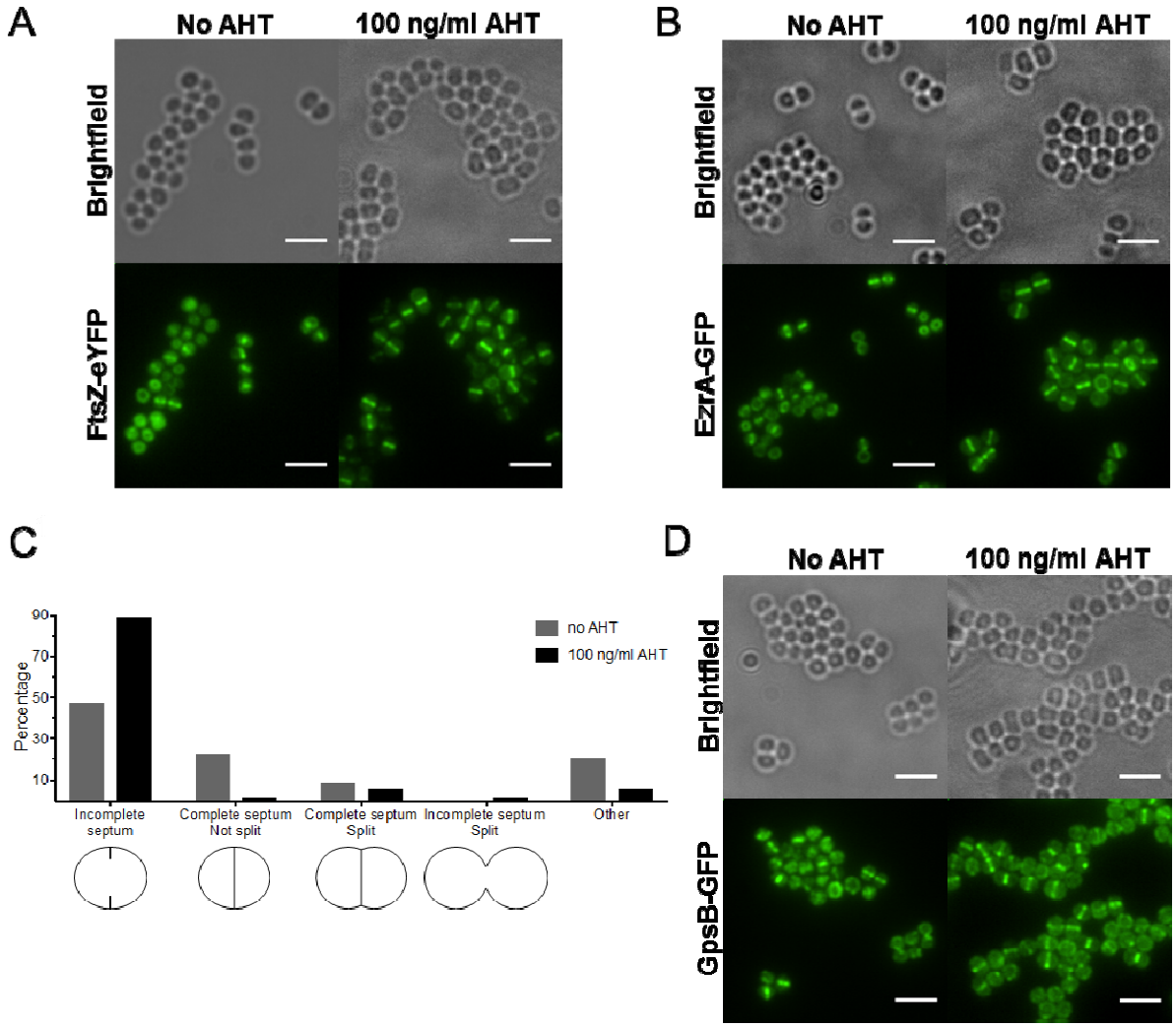

805

806 **Fig 8** SosA does not impair the localization of cell-division proteins and septum formation

807 initiation. (A) Localization of FtsZ-eYFP in SJF4694 (JE2 pSosA pCQ11-FtsZ-eYFP) grown in the

808 absence and presence of 100 ng/ml of AHT for 45 min. (B) EzrA-GFP localization in SJF4697 (JE2

809 pSosA *ezrA-gfp*+) grown in the absence or presence of 100 ng/ml AHT for 45 min. (C) Percentages

810 of JE2 pSosA cells exhibiting incomplete, complete, complete split, or incomplete split septa (n =

811 573 for no AHT, n = 607 for 100 ng/ml of AHT; organisms either isolated or co-adhered in pairs;

812 other represents staining in indistinct shape) after incubation with or without AHT for 45 min. (D)

813 GpsB-GFP localization in SJF700 (JE2 pSosA *gpsB-gfp*+) grown in the absence or presence of 100

814 ng/ml of AHT for 45 min. All fluorescence images are average intensity projections. All scale bars

815 represent 3 um.

816

817 **Figure 9**

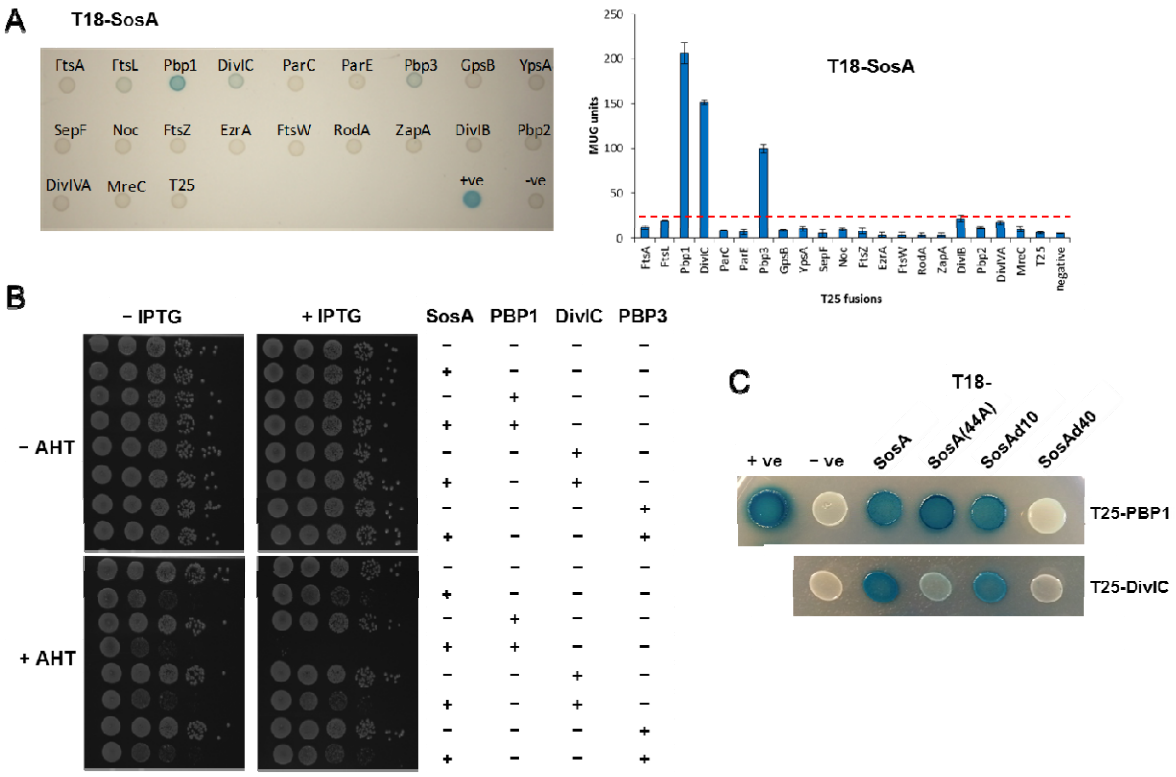

818

819

820 **Fig 9** SosA interaction with the central divisome components. (A) Analysis of the protein

821 interactions between SosA and a panel of *S. aureus* cell-division or cell wall-synthesis proteins

822 using the bacterial two-hybrid system. T18 and T25 are domains of an adenylate cyclase enzyme,

823 and the “T18-SosA” and “T25 fusions” labels indicate the fusions between the C-terminus of the
824 T18 adenylate cyclase fragment to the N-terminus of SosA and the T25 fusions to the cell-division
825 proteins. *Left*: Interactions between the *S. aureus* cell-division proteins fused to T25 and *S. aureus*
826 SosA fused to T18, wherein 10 µl of a 1:100 dilution of overnight culture of co-transformed
827 BTH101 were spotted onto minimal medium containing 150 µg/ml of X-gal and incubated at 30°C
828 for 36 h. +ve, T25-zip + T18-zip; -ve, pKT25 + pUT18C. *Right*: β–Galactosidase activity of
829 interactions between *S. aureus* T18-SosA and cell-division proteins (T25 fusions). Activity is
830 displayed as the mean of three independent measurements of β–galactosidase activity, in MUG
831 (4-methylumbelliferyl-β-D-galactopyranoside) units, for each co-transformant. Error bars
832 represent the standard deviation. Positive interactions are considered to be at least four times
833 higher than the activity level for the negative control, and this cut-off level is represented by the
834 red line in the bar chart. (B) Assessment of the plating efficiency of *S. aureus* JE2 upon
835 concomitant overexpression of *sosA* (pSosA, AHT-inducible) and *pbpA* (pPBP1) or *divIC* (pDivIC) or
836 *pbpC* (pPBP3) controlled by IPTG (+). (-) denotes the vector controls. Cells were grown
837 exponentially to an OD_{600} of 0.5, serially 10-fold diluted, and plated on TSA plates containing 100
838 ng/ml AHT and 0.2 mM IPTG where indicated. The plates were incubated overnight at 37°C and
839 imaged. (C) Interactions of T18 fusions to SosA, SosA(44A), SosAd10 and SosAd40 with T25-PBP1
840 or T25-DivIC. 10 µl of a 1:100 dilution of overnight cultures of co-transformed BTH101 were
841 spotted onto LB containing 150 µg/ml of X-gal and incubated at 30°C for 24 h. +ve and –ve
842 denotes positive and negative interaction controls, respectively.
843
844 **Figure 10**

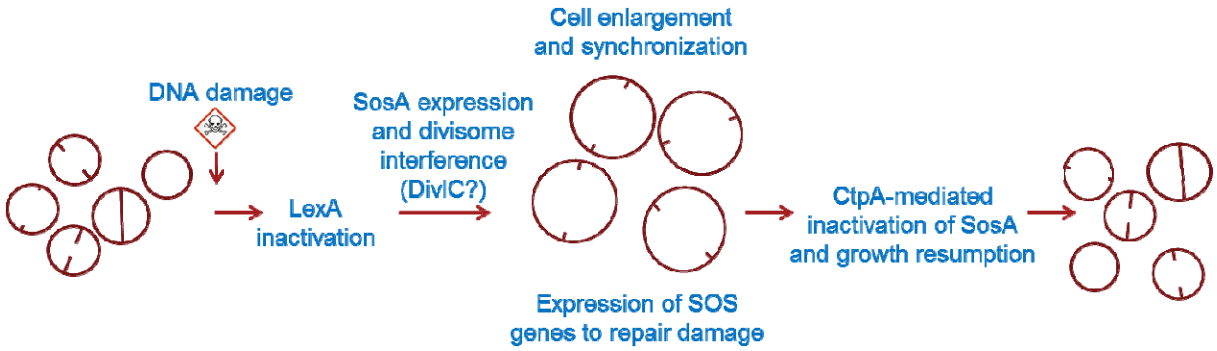

845

846 **Fig 10** Proposed model for a regulated survival strategy for *S. aureus* upon DNA damage. As part of
847 the SOS response, SosA is produced and, by a membrane-localized activity, corrupts normal cell-
848 division activity, likely via an interaction with essential divisome components. In effect, cells are
849 still able to initiate septum formation but are unable to complete it, leading to synchronization of
850 the cell population. This provides a spatio-temporal window for paralleled SOS response-regulated
851 DNA-repair activity. At the same time, the cell size increases due to off-septal activity of
852 peptidoglycan-synthesis enzymes. As the SOS response diminishes, the cellular concentration of
853 SosA is lowered, directly or indirectly, by the proteolytic activity of CtpA. At this stage, septa are
854 allowed to complete and normal growth/division continues.

855

856 **Supplemental Material**

857 6 supplementary figures, 1 supplementary table, 3 supplementary movies.

858 **Legends for supplemental material**

859 **Fig. S1** Percent identity matrix for staphylococcal SosA proteins. Pairwise identity scores for the
860 proteins included in the alignment in Figure 1 were obtained by the Clustal 2.1 algorithm.

861 **Fig. S2** (A) Detection by western blot of DNA-damage induced expression of SosA. SosA being
862 detected in wildtype *S. aureus* 8325-4 and the complemented strain, while being absent in the
863 *sosA* deletion mutant following 1 h of MMC treatment (1 µg/ml). Also displayed is the time-
864 dependent expression of SosA in *S. aureus* JE2 post MMC addition (1 µg/ml) in comparison to the
865 corresponding *sosA* deletion mutant. (B and C) Phenotypic complementation of the *sosA* deletion
866 mutant. The phenotypes of *S. aureus* 8325-4Δ*sosA* were restored back to wildtype by
867 chromosomal integration of a copy of the *sosA* gene under its native promoter (*S. aureus* 8325-
868 4Δ*sosA*-compl.) when evaluated for changes in cell density and viability (B) and cell size assessed
869 by flow cytometry (C) during challenge with MMC (1 µg/ml). Mean FSC-A values are indicated
870 below histograms. Cells were grown exponentially prior to addition of MMC at an OD_{600} of 0.05.
871 (D) Effect of different truncated SosA variants on *S. aureus* cell size. Evaluation of cell size
872 distribution was performed by flow cytometry (FSC-A) of *S. aureus* RN4220 containing expression
873 plasmids encoding full length SosA or C-terminally truncated variants of the protein. Mean FSC-A
874 values are indicated below histograms. Cells were grown exponentially prior to induction with 100
875 ng/ml of AHT and analyzed at indicated time points. (E) Western blot of accumulation in *S. aureus*
876 JE2 of SosA, SosAd10, SosA(44A), and SosAd10(44A) expressed from respective plasmid constructs
877 for 1 h with 200 ng/ml AHT.

878 **Fig. S3** Hypersusceptibility of an *S. aureus* JE2 *ctpA* mutant to SosA-mediated growth inhibition.
879 Plating efficiency of the *S. aureus* JE2-*ctpA*(−erm) mutant transformed with both SosA and CtpA
880 expression plasmids (+) or vector controls (-) at different inducer concentrations; AHT for SosA and
881 IPTG for CtpA. Cells were grown exponentially to an OD_{600} of 0.5, serially 10-fold diluted, and
882 plated on TSA plus indicated inducer concentrations followed by incubation overnight at 37°C
883 before imaging.

884 **Fig. S4** SosA halts septum completion. Localization of (A) FtsZ-eYFP in SJF4693 (JE2 pRAB12-*lacZ*
885 pCQ11-FtsZ-eYFP), (B) EzrA-GFP in SJF4696 (JE2 pRAB12-*lacZ ezrA-gfp*+) and (D) GpsB-GFP in
886 SJF4699 (JE2 pRAB12-*lacZ gpsB-gfp*+) grown in the absence and presence of 100 ng/ml of AHT for
887 45 min. Fluorescence images are average intensity projections. Scale bars represents 3 µm. (C)
888 Fluorescence microscopy images of JE2/pSosA grown in the absence or presence of 100 ng/ml of
889 AHT for 45 min and labeled with HADA for 5 min. Images are average intensity projections. Scale
890 bars represents 3 µm. (E) 3D-SIM Z-stack images of JE2/pSosA grown with 100 ng/ml of AHT for 45
891 min and labelled with Alexa Fluor 647 NHS ester. (i) A cell with initiated septum formation and (ii)
892 a cell splitting into daughter cells without finishing a septal disc. Scale bars represents 0.5 µm.

893 **Fig. S5** Assessment of the plating efficiency of *S. aureus* strain JE2 upon expression of *sosA* (pSosA,
894 AHT-inducible) and concomitant overexpression of PBP1 (*pbpA*) or a PBP1 transpeptidase mutant
895 PBP1* (*pbpA**) (A), PBP1 (*pbpA*) and in comparison to SosA(44A) (B), MurJ (C), and FtsL (D).
896 Inducer concentrations for SosA (and SosA(44A)) were 50 ng/ml (panels A-C) and 150 ng/ml AHT
897 (panel D). Co-expression proteins were induced by 0.2 mM IPTG. (+) denotes protein encoding
898 vectors, (-) denotes empty vector controls. In all panels, cells were grown exponentially to an
899 OD_{600} of 0.5, serially 10-fold diluted, and plated on TSA with/without inducers followed by
900 incubation overnight at 37°C before imaging.

901 **Fig. S6** Uncropped western blots relating to Figure 7 and Figure S2.

902 **Movie S1.** Time-lapse microscopy of *S. aureus* JE2 WT and *sosA* mutant upon MMC exposure.
903 **Movie S2.** Time-lapse microscopy of *S. aureus* JE2 cells overexpressing SosA.

904 **Movie S3.** Time-lapse microscopy of *S. aureus* JE2 cells overexpressing SosAd10.